Johansen A., Jacquet E., Cuzzi J. N., Morbidelli A., and Gounelle M. (2015) New paradigms for asteroid formation. In *Asteroids IV* (P. Michel et al., eds.), pp. 471–492. Univ. of Arizona, Tucson, DOI: 10.2458/azu_uapress_9780816532131-ch025.

New Paradigms for Asteroid Formation

Anders Johansen
Lund University

Emmanuel Jacquet
Canadian Institute for Theoretical Astrophysics, University of Toronto

Jeffrey N. Cuzzi
NASA Ames Research Center

Alessandro Morbidelli
Lagrange Laboratory, Université Côte d'Azur, Observatoire de la Côte d'Azur, CNRS

Matthieu Gounelle
Muséum National d'Histoire Naturelle, Institut Universitaire de France

Asteroids and meteorites provide key evidence on the formation of planetesimals in the solar system. Asteroids are traditionally thought to form in a bottom-up process by coagulation within a population of initially kilometer-scale planetesimals. However, new models challenge this idea by demonstrating that asteroids of sizes from 100 to 1000 km can form directly from the gravitational collapse of small particles that have organized themselves in dense filaments and clusters in the turbulent gas. Particles concentrate passively between eddies down to the smallest scales of the turbulent gas flow and inside large-scale pressure bumps and vortices. The streaming instability causes particles to take an active role in the concentration, by piling up in dense filaments whose friction on the gas reduces the radial drift compared to that of isolated particles. In this chapter we review new paradigms for asteroid formation and critically compare them against the observed properties of asteroids as well as constraints from meteorites. Chondrules of typical sizes from 0.1 to 1 mm are ubiquitous in primitive meteorites and likely represent the primary building blocks of asteroids. Chondrule-sized particles are nevertheless tightly coupled to the gas via friction and are therefore hard to concentrate in large amounts in the turbulent gas. We review recent progress on understanding the incorporation of chondrules into the asteroids, including layered accretion models where chondrules are accreted onto asteroids over millions of years. We highlight in the end 10 unsolved questions in asteroid formation where we expect that progress will be made over the next decade.

1. INTRODUCTION

The solar system contains large populations of pristine planetesimals that have remained relatively unchanged since their formation. Our proximity to the asteroid belt provides astronomers, planetary scientists, and cosmochemists access to extremely detailed data about asteroid compositions, sizes, and dynamics. Planetesimals are the building blocks of both terrestrial planets and the cores of the giant planets, as well as the super-Earths (with various degrees of gaseous envelopes) that are now known to orbit around a high fraction of solar-type stars (*Fressin et al.,* 2013). The formation of planetesimals is thus a key step toward the assembly of planetary systems, but many aspects of the planetesimal formation process remain obscure.

Recent progress in understanding planetesimal formation was triggered by two important realizations. The first is that macroscopic dust particles (millimeter or larger) have poor sticking properties. Laboratory experiments and coagulation models show that it is difficult to form planetesimals by direct sticking of silicate particles, most importantly because particle growth stalls at millimeter sizes where the particles bounce off each other rather than stick (*Güttler et al.,* 2010). While some particle growth is still possible at relatively high collision speeds, due to the net transfer of mass from small impactors onto large targets (*Wurm et al.,* 2005; *Windmark et al.,* 2012a), the resulting growth rate is too low to compete with the radial drift of the particles.

The second important realization is that particles are concentrated to very high densities in the turbulent gas flow.

This idea is not new — *Whipple* (1972) already proposed that large-scale pressure bumps can trap particles, as their radial drift speed vanishes in the pressure bump where the radial pressure gradient is zero. However, the advent of supercomputing led to the discovery and exploration of a large number of particle concentration mechanisms. Large-scale axisymmetric pressure bumps, akin to those envisioned by *Whipple* (1972), have been shown to arise spontaneously in simulations of protoplanetary disk turbulence driven by the magnetorotational instability (*Johansen et al.,* 2009a; *Simon et al.,* 2012). Particle densities reach high enough values inside these pressure bumps to trigger gravitational collapse to form planetesimals with sizes up to several 1000 km (*Johansen et al.,* 2007, 2011; *Kato et al.,* 2012). The baroclinic instability, which operates in the absence of coupling between gas and magnetic field, leads to the formation of slowly overturning large-scale vortices (*Klahr and Bodenheimer,* 2003), which can act as dust traps in a similar way as pressure bumps (*Barge and Sommeria,* 1995).

In the streaming instability scenario the particles play an active role in the concentration (*Youdin and Goodman,* 2005). The relative motion between gas and particles is subject to a linear instability whereby axisymmetric filaments of a slightly increased particle density accelerate the gas toward the Keplerian speed and hence experience reduced radial drift. This leads to a runaway pileup of fast-drifting, isolated particles in these filaments (*Johansen and Youdin,* 2007). The densities achieved can be as high as 10,000× the local gas density (*Bai and Stone,* 2010; *Johansen et al.,* 2012), leading to the formation of planetesimals with characteristic diameters of 100–200 km for particle column densities relevant for the asteroid belt, on a timescale of just a few local orbital periods.

A concern about large-scale particle concentration models is that typically very large particles are needed for optimal concentration (at least decimeter in size when the models are applied to the asteroid belt). Chondrules of typical sizes from 0.1 to 1 mm are ubiquitous in primitive meteorites, but such small particles are very hard to concentrate in vortices and pressure bumps or through the streaming instability. One line of particle concentration models has nevertheless been successful in concentrating chondrules. Swiftly rotating low-pressure vortex tubes expel particles with short friction times (*Squires and Eaton,* 1990, 1991; *Wang and Maxey,* 1993). This was proposed to explain the characteristic sizes and narrow size ranges of chondrules observed in different chondrites (*Cuzzi et al.,* 2001) and leads to the formation of 100-km-scale asteroids from rare high-density concentrations (*Cuzzi et al.,* 2008, 2010). However, the evaluation of the probability for such high-density concentrations to occur over sufficiently large scales depends on scaling computer simulations to the very large separations between the energy injection scale and the dissipation scale relevant for protoplanetary disks; *Pan et al.* (2011) found that the particle clustering gets less contribution from the addition of consecutively larger scales than originally thought in the model of *Cuzzi et al.* (2008, 2010).

Therefore the incorporation of chondrules into the asteroids is still an unsolved problem in asteroid formation. This is one of the main motivations for this review. We refer the readers to several other recent reviews on the formation of planetesimals that provide a broader scope of the topic beyond asteroid formation (e.g., *Cuzzi and Weidenschilling,* 2006; *Chiang and Youdin,* 2010; *Johansen et al.,* 2014).

The review is organized as follows. The first two sections discuss the constraints on asteroid formation from the study of meteorites (section 2) and asteroids (section 3). In section 4 we review laboratory experiments and computer simulations of dust coagulation to illustrate the formidable barriers that exist to planetesimal formation by direct sticking. The turbulent concentration model, in which chondrule-sized particles are concentrated at the smallest scales of the turbulent gas flow, is discussed in section 5. Section 6 is devoted to particle concentration in large-scale pressure bumps and through streaming instabilities. In section 7 we discuss layered accretion models where the chondrules are accreted onto planetesimals over millions of years. Finally, in section 8 we pose 10 open questions regarding the formation of asteroids on which we expect major progress in the next decade.

2. CONSTRAINTS FROM METEORITES

Meteorites provide a direct view of the solid material from which the asteroids accumulated, while the crystallization ages of the component particles and the degree of heating and differentiation of the parent bodies give important information about the timescales for planetesimal formation in the solar system.

Meteorites may be broadly classified in two categories (*Weisberg et al.,* 2006): primitive meteorites (also known as chondrites) and differentiated meteorites. Chondrites, which make up 85% of the observed falls, are basically collections of millimeter- and submillimeter-sized solids, little modified since agglomeration and lithification (compression) in their parent bodies. They exhibit nonvolatile element abundances comparable to the solar photosphere's (*Palme and Jones,* 2005). Differentiated meteorites derive from parent bodies that underwent significant chemical fractionations on the scale of the parent body, resulting in the asteroid-wide segregation of an iron core and silicate mantle and crust. In the process, differentiated meteorites have lost not only their accretionary (presumably chondritic) texture, but also their primitive chemical composition; depending on which part of the parent body they sample, some may be essentially pure metal (the iron meteorites) while others are essentially metal-free (the achondrites).

It is among the components of chondrites that the oldest solids of the solar system, the refractory inclusions (*Krot et al.,* 2004; *MacPherson,* 2005), in particular calcium-aluminium-rich inclusions (CAIs), have been identified. Their age of 4567.3 ± 0.16 m.y. (*Connelly et al.,* 2012) marks the commonly accepted "time zero" of the solar system. But the ubiquitous components of chondrites are the eponymous

chondrules (*Hewins et al.,* 2005; *Connolly and Desch,* 2004), which are millimeter-sized silicate spherules presumably resulting from transient (and repeated) high-temperature episodes in the disk, but whose very nature remains a longstanding cosmochemical and astrophysical enigma (*Boss,* 1996; *Desch et al.,* 2012). All these components are set in a fine-grained matrix consisting of amorphous and crystalline grains native to the disk as well as rare presolar grains (*Brearley,* 1996). While compositionally primitive, chondrites may have undergone some degree of thermal metamorphism, aqueous alteration, and shock processing on their parent body.

Despite their general petrographic similarity and roughly solar composition, chondrites are actually quite variable, and 14 distinct chemical groups have been recognized so far, each of which is believed to represent a single parent body — sometimes with supporting evidence from cosmic-ray exposure ages (*Eugster et al.,* 2006) — or at least a family of parent bodies formed in the same nebular reservoir (i.e., a compositionally distinctive space-time section of the disk). There are various levels of affinities between these groups (e.g., clans, classes) but we will be content here to distinguish carbonaceous chondrites (henceforth "CCs," comprising the CI, CM, CO, CV, CK, CR, CH, and CB groups) from noncarbonaceous chondrites [henceforth "EORs," as they include the enstatite (EH, EL), ordinary (H, L, LL), and Rumuruti (R) chondrite groups]. Carbonaceous chondrites are more primitive in the sense that they have a solar Mg/Si ratio and a ^{16}O-rich oxygen isotopic composition closer to that of the Sun (e.g., *Scott and Krot,* 2003). Noncarbonaceous chondrites, although poorer in refractory elements, are more depleted in volatile elements, have subsolar Mg/Si ratios and a more terrestrial isotopic composition for many elements (*Trinquier et al.,* 2009). EORs have generally undergone thermal metamorphism (see Fig. 1), while aqueous alteration has been prevalent in CCs (*Huss et al.,* 2006; *Brearley,* 2003), but again there are exceptions.

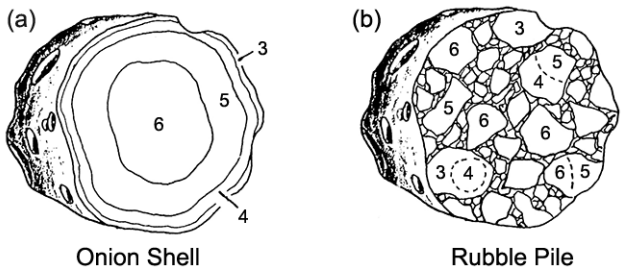

Fig. 1. (a) Initial state of a parent body with a radius of 100 km, which was initially homogeneous throughout, after heating by ^{26}Al. The proportions of the least (3) to most (6) altered material are constrained by meteorite statistics. (**b**) The same body after catastrophic fragmentation and reassembly as a rubble pile with some highly altered material now near the surface. This body is then cratered by subsequent impacts, releasing samples of all metamorphic grades (adapted from *Scott and Rajan,* 1981).

2.1. Primary Texture and Aerodynamic Sorting

The texture of most chondrites has been reworked by impact fragmentation and erosion on their parent body. However, rare pieces of CM and CO chondrites have been found, referred to as "primary texture" (*Metzler et al.,* 1992; *Brearley,* 1993), which seem to retain the nature of a prebrecciated body. Primary texture appears to consist of nothing but dust-rimmed chondrules of very similar properties, loosely pressed together.

The constituents of most chondrites appear well-sorted by size, with strong mean size differences from one group to another (*Brearley and Jones,* 1998). Whether these differences arise from some regionally or temporally variable bouncing-barrier (*Jacquet,* 2014a), some aerodynamic sorting process (sections 5 and 7), or some aspect of the mysterious chondrule-formation process itself, they provide an important clue to primary accretion. *Hezel et al.* (2008) have emphasized the need for better particle counting statistics, and indeed one recent chondrule size distribution measurement taken from Allende, of a far larger sample than analyzed previously (*Fisher et al.,* 2014), points to a distribution substantially broader for that chondrite than previously reported.

Aerodynamic sorting has been suggested often as an important factor in selecting for the contents of primary texture (see *Cuzzi and Weidenschilling,* 2006, for a review). Comparing the aerodynamical friction time of objects of greatly different density, such as silicate and metal grains, shows that their friction times are quite similar in the least-altered meteorites (*Dodd,* 1976; *Kuebler et al.,* 1999), suggesting that asteroids selectively incorporated components with specific aerodynamical properties (we discuss this further in section 3.3).

2.2. The Abundance and Distribution of Aluminum-26 and Iron-60

The melting of the parent bodies of differentiated meteorites puts important constraints on the timescale for planetesimal formation in the asteroid belt. While electromagnetic heating (*Sonett and Colburn,* 1968) or impact heating (*Keil et al.,* 1997) have been considered in the literature, the most likely source of planetesimal heating is the decay of the short-lived radionuclides (SLRs) ^{26}Al (with mean lifetime τ = 1.0 m.y.) and ^{60}Fe (τ = 3.7 m.y.) (*Urey,* 1955). Depending on their respective initial abundance, and on the time of planetesimal accretion, both could have significantly contributed to planetesimal heating. Additionally, short-lived nuclides provide crystallization ages that can be calibrated using a long-lived radionuclide decay system such as Pb-Pb, under the assumption that the short-lived radionuclide was homogeneously distributed in the solar protoplanetary disk.

The content of SLRs in CAIs is usually identified with that of the nascent solar system (*Dauphas and Chaussidon,* 2011). Excesses of ^{26}Mg linearly correlating with ^{27}Al content were first observed in an Allende CAI in 1976 (*Lee et al.,*

1976). This isochron diagram demonstrated the presence of ^{26}Al in the nascent solar system. The CAIs from a diversity of chondrite groups formed with an initial $(^{26}Al/^{27}Al)_0$ of roughly 5×10^{-5} (*MacPherson et al.,* 2014). A remarkably tight isochron for CAIs in the CV chondrites was obtained by *Jacobsen et al.* (2008). The deduced $(^{26}Al/^{27}Al)_0$ ratio of $(5.23 \pm 0.13) \times 10^{-5}$ is often considered as the initial value for the solar system and the small dispersion as indicative of a narrow formation interval (≤40,000 yr). However, this interpretation should be limited to the region where the unusually large CV CAIs have formed (*Krot et al.,* 2009). This is especially true since many CAIs are known to have formed without any ^{26}Al (*Liu et al.,* 2012; *Makide et al.,* 2013). This indicates some level of heterogeneity in the ^{26}Al distribution within the region where CAIs formed (assuming that region was unique, which is supported by the ubiquitous ^{16}O enrichment of CAIs compared to, e.g., chondrules). *Larsen et al.* (2011) used bulk magnesium isotopic measurements to suggest that the heterogeneity of ^{26}Al distribution might have reached 80% of the canonical value in the solar protoplanetary disk. However, *Kita et al.* (2013) and *Wasserburg et al.* (2012) argue that the observed variations can be better ascribed to small heterogeneities in the stable isotope ^{26}Mg.

Although the presence of live ^{60}Fe in the early solar system was demonstrated almost 20 years ago (*Shukolyukov and Lugmair,* 1993), the determination of the solar system initial abundance is complicated by the difficulty of obtaining good isochrons for CAIs (*Quitté et al.,* 2007), given their low abundance in Ni. To bypass that difficulty, most measurements were performed on chondrules that are believed to have formed from around the same time as CAIs up to 3 m.y. later (*Connelly et al.,* 2012). High initial $(^{60}Fe/^{56}Fe)_0$ ratios were originally reported in chondrules from unequilibrated ordinary chondrites (UOC), which experienced very little heating or aqueous alteration (e.g., *Tachibana and Huss,* 2003; *Mostefaoui et al.,* 2005; *Tachibana et al.,* 2006). *Telus et al.* (2012) showed that most of these previous data were statistically biased and that most chondrules do not show any ˙Ni excesses indicative of the decay of ^{60}Fe. The high values obtained in older publications could be due to statistical biases related to low counts (*Telus et al.,* 2012) or to thermal metamorphism, which would have led to the redistribution of Ni isotopes (*Chaussidon and Barrat,* 2009). Recently, improved techniques for measuring bulk chondrules in unequilibrated ordinary chondrites have yielded initial solar system values for $(^{60}Fe/^{56}Fe)_0$ of $\approx 1 \times 10^{-8}$ (*Tang and Dauphas,* 2012; *Chen et al.,* 2013). This value is consistent with that inferred from Fe-Ni isotope measurements of a diversity of differentiated meteorites (*Quitté et al.,* 2011; *Tang and Dauphas,* 2012).

In conclusion, it seems that most CAIs formed with an initial ratio $(^{26}Al/^{27}Al)_0$ of roughly 5×10^{-5}, which can be considered in a first approximation as the solar system average or typical initial value. Some heterogeneity was undoubtedly present, but its exact level is still unknown. On the other hand, it is likely that the initial $(^{60}Fe/^{56}Fe)_0$ of the solar system was lower than 1×10^{-8}, although high levels of ^{60}Fe (up to 10^{-6}) have been detected in some components of chondrites. At the time of writing this review, there was no evidence of ^{60}Fe heterogeneity within the solar protoplanetary disk.

2.3. The Origin of Aluminum-26 and Iron-60

The initial solar system ratio $(^{26}Al/^{27}Al)_0$ of roughly 5×10^{-5} is well above the calculated average galactic abundance (*Huss et al.,* 2009). This elevated abundance indicates a last-minute origin for ^{26}Al. Production of ^{26}Al by irradiation has been envisioned in different contexts (e.g., *Lee,* 1978; *Gounelle et al.,* 2006), but fails to produce enough ^{26}Al relative to ^{10}Be (τ = 2.0 m.y.), another SLR whose origin by irradiation is strongly supported by experimental data (*Gounelle et al.,* 2013). This leaves stellar delivery as the only possibility for ^{26}Al introduction in the solar system. Although asymptotic giant branch stars produce elevated amounts of ^{26}Al (*Lugaro et al.,* 2012), it is extremely unlikely that stars at this evolutionary stage are present in a star-forming region (*Kastner and Myers,* 1994). Thus massive stars are the best (unique) candidates for the origin of the solar system's ^{26}Al.

The recently obtained lower estimates for the abundance of ^{60}Fe (see section 2.2) are compatible with a galactic background origin, independently of whether this is calculated crudely using a box model (*Huss et al.,* 2009), or taking into account the stochastic nature of star formation in molecular clouds (*Gounelle et al.,* 2009). However, if the initial ^{60}Fe abundance corresponds instead to a much higher $(^{60}Fe/^{56}Fe)_0$ ratio of $\approx 10^{-6}$, a last-minute origin is needed. Irradiation processes cannot account for ^{60}Fe production because of its richness in neutrons (*Lee et al.,* 1998). The winds of massive stars can also be excluded, given their low abundance in ^{60}Fe. In contrast, supernovae are copious producers of ^{60}Fe, essentially because this SLR is synthesized in abundance during the hydrostatic and explosive phases of such massive stars (*Woosley and Heger,* 2007). Two astrophysical settings have been envisioned so far. In the first (classical) model (*Cameron and Truran,* 1977), the supernova ejecta hits a molecular cloud core and provokes its gravitational collapse (*Boss and Keiser,* 2013) as well as injecting ^{60}Fe and other SLRs. A newer model injects ^{60}Fe in an already formed protoplanetary disk (*Hester et al.,* 2004; *Ouellette et al.,* 2007). In either cases, the supernova progenitor mass is in the range 20–60 $M_\odot$, because too-massive supernovae are extremely rare and very disruptive to their environment (*Chevalier,* 2000). Alternatively, generations of supernovae could have enriched the gas of the giant molecular cloud, so that the solar protoplanetary disk simply inherited the elevated abundances of the birth cloud (*Vasileiadis et al.,* 2013).

All these models suffer from an important difficulty, namely the overabundance of ^{60}Fe in supernova ejecta relative to ^{26}Al. The solar system ^{60}Fe/^{26}Al mass ratio was either 4×10^{-3} or 0.4 depending on the adopted initial ^{60}Fe abundance. In any case, this is well below the ^{60}Fe/^{26}Al mass ratio predicted by supernovae nucleosynthetic models whose variation domain extends from 1.5 to 5.5 for a progenitor mass varying between 20 and 60 $M_\odot$. Heterogeneity in

the composition of supernova ejecta has been proposed as a possible solution to that discrepancy (*Pan et al.,* 2012). However, that variability is limited to a factor of 4, which would help resolve the discrepancy only marginally in the case of the (unlikely) high ^{60}Fe value. Finally, the astrophysical context of any supernova model is difficult to reconcile with observations of star-forming regions (*Williams and Gaidos,* 2007; *Gounelle and Meibom,* 2008). The commonly proposed setting for supernova contamination of a protoplanetary disk or or a dense core is similar to that of the Orion Nebula, where disks are seen within a few tenths of parsec of the massive star θ^1 C Ori. The problem with that setting is that, when θ^1 C Ori will explode in 4 m.y. from now, these disks will have long evaporated or formed planets. New disks or cores will have obviously formed by then, but they will be at the outskirts of the 10-pc-wide HII region created by θ^1 C Ori (*Chevalier,* 1999). At such a distance, the quantity of ^{26}Al delivered into these disks or cores is orders of magnitude lower than the quantity present in the solar system (*Looney et al.,* 2006). In other words, supernova remnants nearby dense phases are extremely rare (*Tang and Chevalier,* 2014). In conclusion, it seems very unlikely that a nearby supernova was close enough to the solar system to provide the known inventory of ^{26}Al.

If the low value of ^{60}Fe inferred from chondrites is correct, then the presence of ^{26}Al remains to be explained. Supernovae can be excluded as they would vastly overproduce ^{60}Fe (see above). The winds of massive stars have long been known to be ^{26}Al and ^{60}Fe-poor (*Arnould et al.,* 1997). In the models of *Gaidos et al.* (2009) and *Young* (2014), ^{26}Al is injected at the molecular cloud phase by the winds from a large number of Wolf-Rayet stars. The problem with these models is that the Wolf-Rayet phase is followed by the supernova explosion, and therefore they produce a large excess of ^{60}Fe relative to ^{26}Al and their respective solar system values. To escape that caveat, *Young* (2014) has argued that Wolf-Rayet stars do not explode as supernovae but directly collapse into black holes. Although this possibility has been theoretically envisioned, the recent observation of a Wolf-Rayet star going supernova shows this is far from being the rule (*Gal-Yam et al.,* 2014). In addition, models considering injection at the global molecular cloud phase cannot account for the observed heterogeneity of ^{26}Al (see section 2.2).

The last class of models considered injection at the scale of single massive stars. *Tatischeff et al.* (2010) have envisioned a single star that escaped from its parent cluster and interacted with a neighboring molecular cloud, injecting ^{26}Al through its dense wind. It is compromised again by the proximity of the Wolf-Rayet phase with the supernova phase. In addition, Wolf-Rayet stars are rare. In contrast, *Gounelle and Meynet* (2012) proposed that ^{26}Al has been injected in a dense shell of mass ~1000 $M_\odot$ collected by the wind of a massive star. Evolutionary models of rotating stars are used, so the injection in the shell starts as early as the entry of the star onto the main sequence, lasts for some million years, and ends well before the supernova explosion. When the collected shell has become dense enough and gravitationally unstable, it collapses and a second generation of stars form that contain ^{26}Al. Detailed calculations have shown that as long as the parent star, called "Coatlicue," is more massive than M_{min} = 32 $M_\odot$, the abundance of ^{26}Al in the shell is equal to or larger than that of the solar system, depending on the mixing efficiency of the wind material with the shell. Because the mixing timescale of the dense shell is comparable to its collapse timescale, a certain level of ^{26}Al heterogeneity is expected (*Gounelle and Meynet,* 2012), in agreement with observations. This model is in line with observations of induced star formation within dense shells around massive stars (*Deharveng et al.,* 2010). Because it corresponds to a common — although not universal — mode of star formation, it implies that the solar system is not the only of its kind to have formed with ^{26}Al, and that early differentiation of planetesimals might have been common in exoplanetary systems. *Gounelle* (2014) has estimated that the occurrence of planetary systems that are rich in ^{26}Al and poor in ^{60}Fe is on the order of 1%.

2.4. Timing of Planetesimal Accretion

Planetesimal accretion itself cannot be dated directly with radioisotopic systems, since the mere agglomeration of different solids incurs no isotopic rehomogenization between different mineral phases. Thus one can only obtain upper limits with the age-dating of preaccretionary components (for chondrites) and lower limits from that of secondary (parent body) processes.

Important and ever-improving constraints have emerged since the publication of *Asteroids III*. In particular, Hf-W systematics of achondrites and irons have evidenced early differentiation, sometimes contemporaneous (within errors) with refractory inclusion formation (*Kruijer et al.,* 2012). This indicates that planetesimal formation started very early in the evolution of the solar system. Intriguingly, *Libourel and Krot* (2007) ascribed some olivine aggregates in chondrites to this first generation of planetesimals [but see *Whattam et al.* (2008) and *Jacquet et al.* (2012a) for the alternative view that these formed in the protoplanetary disk]. The above evidence for early differentiation is consistent with thermal modeling expectations, as the initial abundance of ^{26}Al was sufficient to melt planetesimals, so that chondrites had to be accreted later to be preserved to the present day.

Lower limits on chondrite accretion ages may be obtained from phases precipitated during aqueous alteration (see the chapter by Krot et al. in this volume). *Fujiya et al.* (2013) obtained ages of 4562.5–4563.8 m.y. in CI and CM chondrites [recall the accepted age of CAI formation of 4567.3 ± 0.16 m.y. (*Connelly et al.,* 2012)]. As for non-carbonaceous chondrites, recent Mn-Cr dating of fayalite formed during incipient fluid-assisted metamorphism in the least-metamorphosed LL ordinary chondrites yields an age of $4564.9^{+1.3}_{-1.8}$ m.y. (*Doyle et al.,* 2014). Al-Mg systematics in the mildly metamorphosed H chondrite Sainte Marguerite indicate an age of 4563.1 ± 0.2 m.y. (*Zinner and Göpel,* 2002). Thermal modeling based on ^{26}Al heating of

the H-chondrite parent body (one of the ordinary chondrite groups) constrained by dating of chondrites of different metamorphic degrees indicate accretion ages ranging from 1.8 to 2.7 m.y. after refractory inclusions (see *Gail et al.,* 2014, and references therein), while *Fujiya et al.* (2013) advocate accretion of CI and CM chondrites 3–4 m.y. after "time zero" based on similar calculations. If ^{26}Al really is the heat source behind chondrite alteration, then it would indeed make sense that carbonaceous chondrites, little affected by thermal metamorphism, accreted later than their noncarbonaceous counterparts (*Grimm and McSween,* 1993).

Upper limits are provided by the ages of chondrules. In both carbonaceous and noncarbonaceous chondrites, chondrule Pb-Pb ages in individual meteorites span a range of ~4564–4567 m.y. (*Connelly et al.,* 2012), i.e., 0–3 m.y. after refractory inclusions, with younger ages reported by Al-Mg dating for CR (*Kita and Ushikubo,* 2012) and enstatite chondrite (*Guan et al.,* 2006) chondrules. Little correlation is seen between the age of chondrules and their composition (*Villeneuve et al.,* 2012). The significance of Al-Mg ages for chondrules, in particular in relationship with apparently somewhat older Pb-Pb ages (e.g., *Connelly et al.,* 2012), nevertheless remains uncertain.

To summarize, it seems clear that differentiated planetesimals accreted from the outset of the disk evolution while the known chondrites accreted later in the evolution of the disk (~2–4 m.y. after refractory inclusions), as presumably required to escape differentiation, but the exact chronology of chondrite formation and alteration is still in the process of being firmly established.

2.5. Accretion of Chondrules Directly After Formation?

Alexander et al. (2008) proposed that the retention of sodium, a volatile element, in chondrules during their formation indicated high solid densities in the chondrule-forming regions, up to 7 orders of magnitude above expectations for the solar protoplanetary disk and possibly gravitationally bound (see also *Cuzzi and Alexander,* 2006), although quite in excess of what the proportion of compound chondrules suggest (*Ciesla et al.,* 2004). This raises the possibility that the formation of chondrules and chondrites, respectively, may have been contemporaneous, as also advocated by *Metzler* (2012) based on the existence of "cluster chondrites" comprised of mutually indented chondrules [but see *Rubin and Brearley* (1996) for a criticism of such hot accretion models].

A further argument put forward by *Alexander and Ebel* (2012) is that chondrule populations in different chondrite groups are quite distinct (*Jones,* 2012). Indeed, *Cuzzi et al.* (2010) noted that two populations of particles formed simultaneously at 2 and 4 AU would be well-mixed within 1 m.y. for $\alpha = 10^{-4}$. Here α is the nondimensional measure of the turbulent viscosity and diffusion. Relevant values for protoplanetary disks are discussed further in section 6, but we note here that a value of 10^{-4} corresponds to the conditions that are expected if the mid-plane in the asteroid formation region is stirred by turbulent surface layers (*Oishi et al.,* 2007). This would suggest that chondrules had to accrete rapidly to avoid homogenization. However, we do not know exactly the turbulence level or original space time separations between chondrule-/chondrite-forming locations, as the asteroid belt may have undergone significant reshuffling (*Walsh et al.,* 2011). Chondrite groups vary significantly in bulk composition. This indicates that there has been no thorough mixing of chondrite components, whatever their individual transformations in the intervening time were, over the whole chondrite-formation timescale. So whatever fraction of that time the period between chondrule formation and chondrite accretion actually represents, it is not to be expected that chondrules should have been well-mixed over the different chondrite-forming reservoirs (*Jacquet,* 2014b).

A link between chondrules and matrix is suggested, in the case of carbonaceous chondrites, by complementarity: The bulk meteorite is solar in some respect (e.g., the Mg/Si ratio), but its separate components (chondrules/matrix/refractory inclusions) are not [chondrules have a typically higher Mg/Si than solar while the converse is true for the matrix (*Hezel and Palme,* 2010)]. Complementarity — if verified, as for at least some elements it may reflect analytical biases or parent-body processes (*Zanda et al.,* 2012) — would indicate a genetic relationship between chondrules and matrix, which would have exchanged chemical elements upon formation, a relationship that would not be predicted, e.g., in an X-wind scenario for chondrule formation (*Hezel and Palme,* 2010) in which chondrules and matrix would have formed in different locations. But it does not require immediate accretion of chondrule and matrix. It only requires chondrules and dust grains to have been transported in a statistically similar way, as was likely the case for a large portion of the disk evolution until accretion. Several batches of chondrule + dust may have contributed to a given chondrite-forming reservoir, again provided they suffered no loss of chondrules relative to dust or vice versa (*Cuzzi et al.,* 2005; *Jacquet et al.,* 2012b). This nonetheless does assume that at the stage of chondrule/matrix agglomeration, there was no bias for or against the incorporation of any component (*Jacquet,* 2014a), which may be an important constraint on the accretion process. The problem is that small dust grains are much harder to incorporate into asteroidal bodies than the macroscopic chondrules, due to their strong frictional coupling with the gas. One could nevertheless envision that chondrules and matrix agglomerated together as compound objects (see section 4.2.5) prior to incorporation in asteroidal bodies and/or that matrix-sized dust coagulated with ice into lumps with aerodynamical properties equivalent to chondrules.

So the jury is still out on whether chondrule formation immediately preceded incorporation in a chondrite or not. Given the chondrule age spread of 3 m.y. within individual chondrites (*Connelly et al.,* 2012), as well as the presence of refractory inclusions and presolar grains that would not have survived chondrule-forming events, it is possible that chondrite components did spend up to a few million years as free-floating particles in the gaseous disk prior to accretion.

3. CONSTRAINTS FROM THE ASTEROID BELT

The modern asteroid belt contains only a fraction of its original planetesimal population. However, the shape of the size distribution of the largest asteroids is primordial and gives important insights into the birth sizes of the planetesimals. Asteroid families provide a way to probe whether the asteroids are internally homogeneous or heterogeneous on large scales.

3.1. Asteroid Size Distribution

The observed size distribution of asteroids in the main belt shows a quite steep slope for bodies with diameter D > 100 km and a much shallower slope for smaller bodies (*Bottke et al.,* 2005). A similar change of slope with an elbow at D ~ 130 km is observed in the Kuiper belt population (*Fraser et al.,* 2014).

It was expected that the transition from a steep to a shallower slope is the consequence of the collisional disruption of smaller bodies. However, *Bottke et al.* (2005) reached the opposite conclusion by examining the collisional evolution of the asteroid belt in detail. They used a number of constraints (the total number of catastrophic asteroid families, the survival of the basaltic crust on Vesta, the existence of only 1–2 major basins on that body, etc.) to conclude that the integrated collisional activity of the asteroid belt had to be less than that of the current main-belt population in a putative timespan of 10 G.y. If one supposes that initially the asteroid belt size distribution had a unique slope (the slope now observed for D > 100 km), such a limited collisional evolution is not sufficient to reduce the slope of the size distribution of objects smaller than 100 km down to the observed value, i.e., to create the observed elbow. Therefore, *Bottke et al.* (2005) concluded that the elbow at D ~ 100 km is a fossil feature of the primordial size distribution. For the Kuiper belt, the constraints on the integrated collisional activity are not as tight as for the asteroid belt. Nevertheless, models seem to suggest that collisional evolution alone could not create an elbow at diameters larger than 8 km (*Pan and Sari,* 2005), which is significantly smaller than the observed value.

Morbidelli et al. (2009) failed to produce the elbow at D ~ 100 km in the asteroid belt in collisional coagulation simulations starting from a population of small planetesimals (see Fig. 2). So, having in mind the new models of formation of large planetesimals from self-gravitating clumps of chondrules or larger pebbles and boulders (*Johansen et al.,* 2007; *Cuzzi et al.,* 2008), they proposed that 100 km was the minimal diameter of the original planetesimals. Moreover, not being able to reproduce the current slope of D > 100 km asteroids by mutual collisions between bodies 100 km in size, *Morbidelli et al.* (2009) argued that these large planetesimals were born with a similar slope. However, as we will see in section 7, the current slope can be reproduced by considering the accretion of chondrule-sized particles by 100-km-scale planetesimals during the gaseous disk phase, a process not considered by *Morbidelli et al.* (2009).

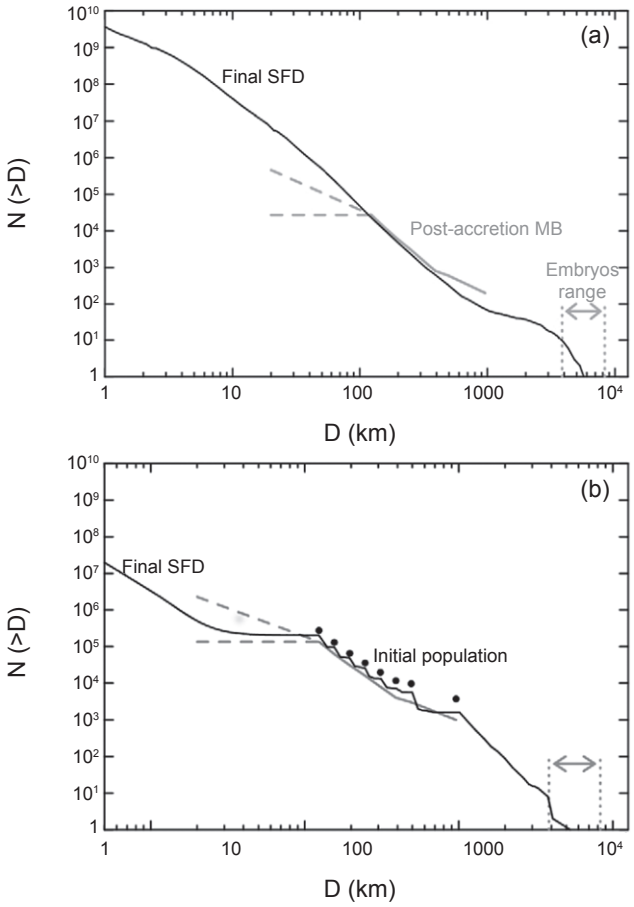

Fig. 2. The cumulative size distribution of asteroids N (>D), as a function of asteroid diameter D, from *Morbidelli et al.* (2009). These coagulation models started with either **(a)** kilometer-sized planetesimals or **(b)** an initial size distribution following the current, observed size distribution of asteroids between 100 and 1000 km in diameter. The gray line shows the current size distribution of asteroids larger than 100 km in diameter. The model with small planetesimals overproduces asteroids smaller than 100 km in diameter (the upper dashed line represents the current size distribution of small asteroids while the lower dashed lines indicates a tighter constraint on the size distribution directly after accretion of the main belt). Starting with large asteroids gives a natural bump in the size distribution at 100 km in diameter, as the smaller asteroids are created in impacts between the larger primordial counterparts.

Weidenschilling (2011) managed to reproduce the elbow at D ~ 100 km in the asteroid belt from collisional coagulation simulations starting from objects 50–200 m in radius. Because of the small size of these objects, collisional damping and gas drag keep the disk very dynamically cold (i.e., with a small velocity dispersion among the objects). Hence, in the simulations of *Weidenschilling* (2011), the elbow at D ~ 100 km is produced by a transition from dispersion-dominated runaway growth to a regime dominated by Keplerian shear, before the formation of large planetary embryos. However, any external dynamical stirring of the population,

for instance due to gas turbulence in the disk, would break this process. Moreover, these simulations are based on the assumption that any collision that does not lead to fragmentation results in a merger, but 100-m-scale objects have very weak gravity and the actual capability of bodies so small to remain bound to each other is questionable. Finally, we stress that the formation of 100-m-scale bodies is an open issue, in view of the bouncing barrier and meter-sized barrier discussed in section 4.

3.2. Snowline Problems

Among the various meteorite types that we know, carbonaceous meteorites (or at least some of them like CI and CM) contain today a considerable amount (5–10%) of water by mass. Evidence for water alteration is widespread, and it is possible that the original ice content of these bodies was higher, close to the 50% value expected from unfractionated solar abundances. Instead, ordinary chondrites contain <2% water by weight (e.g., *Jarosewich,* 1990; *Krot et al.,* 2009); while ordinary chondrites do show signs of water alteration, it is unlikely that they ever contained 50% water ice by mass. This suggests that the parent bodies of these meteorites (CI and CM vs. ordinary) formed on either side of the condensation line for water, also called the snowline. In other words, the snowline was located in the middle of the asteroid belt at the time when the asteroids formed. Earth is also very water poor (some 0.1% by mass, although uncertain by a factor of ~5), suggesting that the planetesimals in its neighborhood were mostly dry and that water was delivered only by the small amount of planetesimals accreted from farther out (*Morbidelli et al.,* 2000; *Raymond et al.,* 2004; *O'Brien et al.,* 2014). The very dry enstatite chondrites have been proposed to arise from an extinct portion of the asteroid belt located between 1.6 and 2.1 AU from the Sun (*Bottke et al.,* 2012).

The problem with this picture is that chondritic bodies accreted late (2–4 m.y. after CAIs) and that the snowline is expected to migrate toward the Sun with time. The temperature of the disk is set by the equilibrium between heating and cooling. In the inner part of the disk, the heating is predominantly due to the viscous friction of the gas in differential rotation around the Sun, so it is related to the gas accretion rate of the star. The cooling rate is governed by how much mass is in the disk in the form of micrometer-sized grains. In *Bitsch et al.* (2015), the snowline is at 2–3 AU only in the earliest phases of disk evolution when the accretion rate is $\dot{M} = 10^{-7}$ $M_\odot$ yr^{-1}, but the snowline migrates to 1–2 AU already after 500,000 yr when the accretion rate drops below $\dot{M} = 10^{-8}$ $M_\odot$ yr^{-1}. These models are probably optimistically warm, because it is assumed that the ratio between the mass in micrometer-sized dust and the mass in gas is 1% (this reflects the solar metallicity but planetesimal accretion should eventually decrease the dust content) and account for the heating produced by stellar irradiation by a star more luminous than our early Sun. According to the observation of the accretion rate of stars as a function of age (*Hartmann et al.,* 1998) and photoevaporation models (*Alexander and Armitage,* 2006), the accretion rate of the star should drop to $\dot{M} = 10^{-9}$ $M_\odot$ yr^{-1} at 2–3 m.y., i.e., at the time of chondrite formation. The fact that there is no sign of primary accretion in the solar system after ~3 m.y. also suggests that the disk disappeared at that time (or that all the solids could have been incorporated into parent bodies at that time — however, accretion of solids is unlikely to reach 100% efficiency). Thus, at the time of chondrite formation, the snowline should have been well inside the inner edge of the asteroid belt, possibly even inside 1 AU. This is at odds with the paucity of water in the ordinary chondrites and in Earth.

A way to keep the disk warm has been proposed recently by *Martin and Livio* (2012, 2013). In their model, a dead zone in the disk, with low turbulent viscosity, becomes very massive and develops gravitational instabilities that heat the gas. The unlimited pileup of gas in the dead zone, however, could be a consequence of a simplified disk transport model, and is not observed in more complex three-dimensional hydrodynamical calculations (*Bitsch et al.,* 2014). Also, the model of *Martin and Livio* (2012) predicts a cold region where ice could condense inside the orbit of Earth, which seems inconsistent with the compositions of Venus and Mercury.

A possible way to keep the asteroid belt ice poor, despite freezing conditions, is to stop the inward flow of icy pebbles in a pressure bump. The inward drift of pebbles is caused by friction with the slower-moving gas (this effect is discussed more in section 6.1). Then, when the nebula cooled locally below the ice condensation temperature, there was no water vapor present to condense, and the planetesimals formed there would have a volatile depletion similar to that achieved in a warm disk. *Bitsch et al.* (2014) explored the effects of viscosity transitions at the snowline (as suggested by *Kretke and Lin,* 2007), but found that only very steep radial gradients in the α parameter allow the formation of a pressure bump. *Lambrechts et al.* (2014) showed that the formation of a proto-Jupiter of about 20 $M_\oplus$ can produce a strong pressure bump just exterior to its orbit. If proto-Jupiter formed at the snowline when the snowline was at the outer edge of the asteroid belt, then its presence would have shielded the asteroid belt and the terrestrial planet region from the flow of icy pebbles, while small silicate dust and chondrules would remain for longer times in the asteroid belt due to their slow radial drift.

3.3. Are Asteroids Internally Homogeneous?

The possibility that the asteroids grew incrementally by layered accretion of chondrules (section 7) implies that asteroids are internally heterogeneous, in the most extreme case with a chondritic surface layer residing on a differentiated interior. We discuss here briefly whether such internal heterogeneity is supported by observations of the asteroid belt. *Burbine et al.* (2002) note that 100–150 distinct meteorite parent bodies, three-fourths of them differentiated, are represented in the meteorite collection. However, this sample is biased toward the sturdy irons and against the weaker, never-melted primitive chondrites.

Differentiation is a constraint on formation age. Most studies have suggested that sizeable asteroids forming $<10^6$ yr after CAIs are almost certain to have thoroughly melted, but those that formed more than 2 m.y. after CAIs may have escaped melting except near their centers. More recent work paints a more complicated picture (see the chapter by Scheinberg et al. in this volume). Specifically, the Allende parent body, source of primitive CV3 chondrites, is thought to have melted near its center, as evidenced by the paleomagnetism detected in these meteorites (*Elkins-Tanton et al.,* 2011); other CV chondrites may show a similar signal (*Weiss et al.,* 2010). This suggests that the CV parent body was differentiated in its interior, but preserved an undifferentiated chondritic layer. Other authors have ascribed the magnetic field in the CV chondrites to impacts (e.g., *Wasson et al.,* 2013).

Modeling of the buoyancy of silicate melts of different composition suggests that, for C-type composition, melt might be dense and remain stable at depth, but for S-type (OC) compositions, and certainly for enstatite compositions, melt is less dense than surrounding material and will rise to manifest on the surface (*Fu and Elkins-Tanton,* 2014). Thus there might be old, centrally melted C-type asteroids such as the Allende parent body, where the evidence for differentiation remains buried, but the lack of evidence for significant surface melting on most S-type asteroids may argue that most of them remain unmelted and undifferentiated throughout (see the chapter by Scheinberg et al. in this volume) (*Weiss and Elkins-Tanton,* 2013).

We can sample the internal properties of asteroids in two ways: from the observed color and albedo distributions of collisionally disrupted asteroids in families (see also the chapters by Nesvorný et al. and Michel et al. in this volume) and from the meteorites that derive from them (see next paragraph). The Near-Earth Object Wide-field Infrared Survey Explorer (NEOWISE) mission has measured the albedos of a large number of asteroids and families, finding a dichotomy in albedo, roughly corresponding to the classical S- and C-types, that is most evident in the outer main belt. Collisional families cover the entire belt, so they avoid the sampling bias that affects meteorites. Many families have internal albedo distributions that are narrower than the global spread of albedos across families. A similar story is told by observations at visual and near-infrared wavelengths (*Mothé-Diniz and Nesvorný,* 2008). This conclusion is nevertheless complicated by the identification of interlopers in (and exclusion from) the asteroid families. Hence there is an inherent tendency to observe low-albedo variations within asteroid families. In contrast, the Eos family and the Eunomia family have unusually large internal variance (*Mothé-Diniz et al.,* 2005, 2008) and the Eunomia family looks like what an internally differentiated S-type might produce (see discussion in *Weiss and Elkins-Tanton,* 2013).

The three ordinary chondrite groups (H, L, and LL) are each thought to derive from a single parent body, based on a clustering of cosmic-ray-exposure ages of chondrites in each group, as if they were excavated by the same few large impacts (*Eugster et al.,* 2006). The thermal history of the H-chondrite parent body under internal heating by ^{26}Al was modeled by *Trieloff et al.* (2003), *Monnereau et al.* (2013), and *Henke et al.* (2013), who all concluded it was a roughly 100-km-radius body. Chondrites from all three OC groups show different amounts of thermal alteration from this process, designated as metamorphic grades 3–6. Models imply that the H-chondrite parent, at least, first incurred thermal alteration in an "onion-shell" fashion, with the most strongly heated H5/H6 material heated deep in the interior, and then was catastrophically disrupted and reassembled as a rubble pile (see Fig. 1) (*Taylor et al.,* 1987; *Scott et al.,* 2014). The small fractional abundance of minimally altered chondrites (H3/H4; Fig. 1) constrains the accretion of the H-chondrite parent body to have happened quickly — probably faster than 3×10^5 yr (*Henke et al.,* 2013; *Vernazza et al.,* 2014). The constant mass growth rate adopted in *Henke et al.* (2013) is nevertheless not applicable to layered accretion, which results in runaway accretion and deposition of most of the mass toward the end of the growth phase (see further discussion in section 7).

While the major-element chemical compositions, and the oxygen isotopic compositions, of the OC groups differ significantly, there is little or no discernible variation of either chemical or isotopic composition across metamorphic grades in any of the three groups (*Jarosewich,* 1990; *Wood,* 2005; see also Tables 1 and 2 of *Clayton et al.,* 1991). The variation of chondrule size across metamorphic grade is less well studied (A. Rubin, personal communication, 2014).

Dodd (1976) demonstrated that the difference in the aerodynamical friction time between metal grains and silicate chondrules can explain silicate-metal fractionation in the ordinary chondrites. In this picture the LL chondrites are underabundant in metal because the parent body was successfully able to accrete large silicate-rich chondrules [the chondrules in the LL chondrites are larger than those in both H and L chondrites (see, e.g., *Nelson and Rubin,* 2002)]. The oxidation of metallic Fe could have happened as the LL-chondrite parent body accreted water-bearing phyllosilicates (*Rubin,* 2005). In the layered accretion model presented in section 7, asteroids will accrete larger and larger particles as they grow. Metal grains had a more restricted size range and hence a relatively small parent body of the H chondrites would accrete mainly small chondrules together with metal grains. A small size of the H-chondrite parent body is further supported by the low fraction of strongly metamorphosed samples that we have from that group (*Dodd,* 1976). A similar story is told for the enstatite chondrites (*Schneider et al.,* 1998): The EH group has more metal and smaller chondrules than the EL group. This aerodynamical size sorting may be evidence of asteroid growth by layered accretion (section 7) or asteroid formation by turbulent concentration (section 5).

4. DUST GROWTH BY STICKING

Now that we have given an overview of some of the constraints from meteorites and asteroids, we can turn to the theoretical models of planetesimal formation. In this section

we discuss the growth of dust by direct sticking; subsequent chapters discuss gravitational instability models.

4.1. Particle-Gas Interaction

The dynamical behavior of a particle in gas depends on both its size and density, as determined by its friction time τ_f in the nebula gas (*Whipple,* 1972; *Weidenschilling,* 1977a). For particles smaller than the gas molecule mean free path (approximately 10–100 cm in the asteroid-belt region, depending on the uncertain value of the gas density), the friction time is

$$\tau_f = \frac{a\rho_\bullet}{v_{th}\rho_g} \quad (1)$$

where a and $\rho_\bullet$ are the particle radius and density, and v_{th} and ρ_g are the gas thermal speed and mid-plane density. The thermal speed of the gas molecules is in turn connected to the isothermal sound speed through $v_{th} = \sqrt{8/\pi}c_s$. The Stokes number St is defined as $St = \Omega\tau_f$, where Ω is the (local) orbital frequency of the protoplanetary disk. The translation from Stokes number to particle size follows

$$a = \frac{(2/\pi)\Sigma_g\, St}{\rho_\bullet} \approx 80\ St\ f_g(r)\left(\frac{r}{2.5\ AU}\right)^{-1.5}\ cm \quad (2)$$

Here $\Sigma_g = \sqrt{2\pi}\rho_g H_g$ is the gas column density and $f_g(r)$ a parameter that sets gas depletion relative to the minimum mass solar nebula (MMSN) as a function of semimajor axis r. We set in the second equality $\rho_\bullet = 3.5$ g cm^{-3}, relevant for chondrules. The Stokes number controls many aspects of dust dynamics. Particles of larger Stokes numbers couple increasingly to larger, longer-lived, and higher-velocity eddies in nebula turbulence, thus acquiring larger relative velocities. Solutions for particle velocities have been developed by *Voelk et al.* (1980) and *Mizuno et al.* (1988), including closed-form analytical expressions by *Cuzzi and Hogan* (2003) and *Ormel and Cuzzi* (2007). Importantly, the Stokes number also controls the degree of sedimentation, with the scale height of the sedimented mid-plane layer, H_p, given by

$$H_p = H_g\sqrt{\frac{\alpha}{St + \alpha}} \quad (3)$$

Here H_g is the gas scale-height and α is a measure of the turbulent diffusion coefficient D normalized as $D = \alpha c_s H_g$ (see *Johansen et al.,* 2014, for references). Significant sedimentation can occur when $St \geq \alpha$. Chondrules of millimeter sizes have a Stokes number of $St \sim 10^{-3}$; hence chondrules will only settle out of the gas if $\alpha \ll 10^{-3}$.

4.2. Dust Growth

The study of dust growth has been an extremely active field, both experimentally and numerically, since *Asteroids III*. Subsequent reviews were presented by *Dominik et al.* (2007), *Blum and Wurm* (2008), and *Chiang and Youdin* (2010); the older review by *Beckwith et al.* (2000) is also valuable for basics. Two very recent overview chapters presenting both the basic physics and selected recent highlights are *Johansen et al.* (2014) and *Testi et al.* (2014); for efficiency we build on those chapters and here emphasize specifics relevant to asteroid formation.

4.2.1. Sticking. Particles can stick if their relative kinetic energy exceeds certain functions of the surface energy of the material, which depends on composition. At the low relative velocities for small monomers (0.1–10 μm) under nebula conditions, both ice and silicate particles stick easily and form loose, porous aggregates. The process continues until the aggregates are at least 100 μm in radius. Aggregates can continue to grow and stick at larger velocities, if their open structure is able to deform and dissipate energy (*Wada et al.,* 2009). The entire process of growth beyond roughly 100 μm fluffy aggregates depends on just how much these aggregates can be compacted by their mutual collisions. Recent studies that concentrate on icy particles outside the snowline have argued that the high surface energy of ice prevents significant compaction from occurring (and keeps relative velocities small) until particles have grown to extremely large size — hundreds of meters — with extremely low density (*Okuzumi et al.,* 2012).

4.2.2. Bouncing. The surface energies of silicates are much smaller than those of ice, so it is easy for even millimeter-sized silicate particles to compact each other in mutual collisions. Relative velocities large enough to cause compaction and bouncing are acquired by roughly millimeter-sized silicate particles in nebula turbulence. Coagulation modeling by *Zsom et al.* (2010), consistent with experiments (*Güttler et al.,* 2010; *Weidling et al.,* 2012), revealed a bouncing barrier in this size range where growth of silicate aggregates by sticking ceased. This new barrier joins the long-known fragmentation barrier and radial drift barrier, which, even if the bouncing barrier can be breached, tend to frustrate growth in the asteroid-belt region beyond decimeter to meter size (*Brauer et al.,* 2008; *Birnstiel et al.,* 2010, 2011).

4.2.3. Fragmentation. A simple critical velocity v_{frag} can be used to refer to fragmentation of two comparable masses. This approach has been modified in some treatments to include some mass transfer by a smaller projectile hitting a larger target at high velocity, even if the projectile is destroyed and some mass is ejected from the target (*Wurm et al.,* 2005). An alternate approach is to treat the fragmentation threshold as a critical kinetic energy per unit mass Q^*, which can be thought of as a critical velocity squared for same-sized particles (*Stewart and Leinhardt,* 2009). The latter treatment automatically accounts for particle size differences and thus allows accretion of small particles to proceed at collision velocities much higher than the nominal $v_{frag} \sim \sqrt{Q^*}$. *Stewart and Leinhardt* (2009) treated solids as weak rubble piles, all calibrated using experimental work by *Setoh et al.* (2007). These expressions allow for the higher efficiency of low-velocity collisions in fragmentation than for hypervelocity impacts. For particles made of small silicate grains, a value of Q^* on the order of 10^4 cm^2 s^{-2} is suggested, with an

associated $v_{frag} \sim 1$ to several meters per second, for weak centimeter- to meter-sized aggregates (*Schräpler et al.,* 2012; *Stewart and Leinhardt,* 2009; *Wada et al.,* 2009, 2013) or even less (*Beitz et al.,* 2011).

4.2.4. Lucky particles. The bouncing barrier, in preserving most of the available solids at small sizes, may provide a target-rich environment for growth of much larger "lucky" particles, which experience few, or low-velocity, collisions and avoid destruction while steadily growing from much smaller particles to large sizes (*Windmark et al.,* 2012a,b; *Garaud et al.,* 2013; *Drążkowska et al.,* 2013). However, *Windmark et al.* (2012a,b) and *Garaud et al.* (2013) did not include radial drift, which is important because the growth time for these lucky particles greatly exceeds the drift time to the Sun. *Drążkowska et al.* (2013) removed the radial drift problem with a pressure bump at the edge of a dead zone, and still found that the total number of meter-sized particles they could produce in 3×10^4 yr was in the single digits. An isolated particle cannot trigger collective effects such as the streaming instability (section 6), but can only keep growing by sweep-up. *Johansen et al.* (2008) and *Xie et al*. (2010) have modeled this "snowball" stage and find that growth in this fashion is extremely slow unless the nebula turbulent α is very low, because the small feedstock particles are vertically diffused to a low spatial density otherwise.

4.2.5. Chondrule rims and chondrule aggregates. The fine-grained component of chondrites is not only found in a featureless background matrix, it is also found rimming individual chondrules and other coarse particles, often filling cavities (*Metzler et al.,* 1992; *Brearley,* 1993; *Cuzzi et al.,* 2005). The origin of these fine-grained rims has been debated (*Lauretta et al.,* 2006). One school of thought regards them as accretionary rims, swept up as a cooled chondrule moves relative to the gas and entrained dust or small aggregates (*MacPherson et al.,* 1985; *Metzler et al.,* 1992; *Bland et al.,* 2011). Matrix and rims were reviewed in depth by *Scott et al.* (1984); among many interesting results, they found evidence that rims were accreted as numerous aggregates of variable mean composition, rather than as monomers. *Rubin* (2011) suggested that carbonaceous chondrites formed in dusty regions of the solar protoplanetary disk and that matrix accumulated into millimeter- to centimeter-sized highly porous dust balls. In this picture, chondrules acquired matrix rims by collisions with these dust balls rather than in collisions with smaller particles.

The accretion of fine-grained rims was modeled by *Morfill et al.* (1998), *Cuzzi* (2004), and *Ormel et al.* (2008). In these models, relative velocities predicted for the nebula environment have been shown to be compatible with sticking and compaction under the theory of *Dominik and Tielens* (1997); *Ormel et al.* (2008) added the effects of interchondrule collisions on further compacting the rims. Ormel et al. found that chondrules that had accreted porous rims of dust between collisions could stick more easily because the porous rims acted as shock absorbers, resulting in composite, centimeter- to decimeter-sized objects, depending on the value of α, formed of rimmed chondrules.

4.2.6. Gravitational scattering barrier. There is one further barrier for particles trying to grow incrementally, by sticking, to kilometer-sized and larger. This gravitational scattering barrier arises because, in turbulence, nebula gas has small density fluctuations associated with pressure and vorticity. These density fluctuations, primarily on large scales, scatter growing planetesimals to achieve high relative speeds (*Laughlin et al.,* 2004; *Nelson and Papaloizou,* 2004; *Nelson and Gressel,* 2010; *Yang et al.,* 2012). The random velocities acquired by 1–10-km-scale planetesimals in this way are sufficient to put them into an erosive, rather than accretionary, regime throughout most of the solar system for a range of the most plausible α values (*Ida et al.,* 2008; *Stewart and Leinhardt,* 2009). *Ormel and Okuzumi* (2013) found that planetesimals need to have radii of 100 km or more to be able to undergo runaway accretion.

Overall, the barriers to formation of 100-km-scale asteroids by incremental growth by sticking appear formidable. For these reasons, a number of models have arisen that avoid these problems with a leapfrog process in which 10–1000-km-scale asteroids form directly from smaller particles stuck at one of these barriers.

5. TURBULENT CONCENTRATION

The leapfrog model, sometimes referred to as turbulent concentration (TC) or turbulent clustering, can in principle make 10–100-km-radius planetesimals directly from chondrule-sized particles. The turbulent concentration model was motivated originally by laboratory and numerical experiments that showed dense particle clusters forming spontaneously in isotropic turbulence, in which the most intense clustering was seen for particles with friction time τ_f equal to the Kolmogorov (or smallest eddy) timescale (*Squires and Eaton,* 1990, 1991; *Wang and Maxey,* 1993; *Eaton and Fessler,* 1994). It was realized that this condition was very closely satisfied under canonical nebula conditions by the very chondrule-sized particles that make up the bulk of primitive chondrites (*Cuzzi et al.,* 1996, 2001).

5.1. A Brief History of Turbulent Concentration Models

What remains uncertain and a subject of current study, as with many properties of turbulence, is just how the laboratory experiments and numerical simulations translate into actual nebula conditions. The flow regime is described by its turbulence Reynolds number $\mathrm{Re} = UL/\nu = \alpha c_s H_g/\nu$, where U and L are some typical velocity and length scale of the flow, and ν is the molecular viscosity. All current experiments and simulations are run at Re far smaller than likely nebula values. *Cuzzi et al.* (2001) noticed that the volume fraction of dense clumps increased with increasing Re and suggested a scaling that would map the behavior to the much higher values of Re relevant for turbulence in protoplanetary disks.

Hogan and Cuzzi (2007) showed that mass-loading feedback of the particle burden on gas turbulence caused

the concentration process to saturate at a mass loading $\Phi = \rho_p/\rho_g \sim 100$, precluding the small, dense clumps advocated by *Cuzzi et al.* (2001). Based on this, *Cuzzi et al.* (2008) advocated gravitational binding and ultimate sedimentation of much larger clumps, on the order of 10^3–10^4 km, with $\Phi \sim$ 10–100. They showed that a long-neglected discovery by *Sekiya* (1983) precludes genuine, dynamical timescale collapse for dense clumps of chondrule-sized particles under plausible conditions. Particles of these sizes and friction times can only sediment slowly toward the center of their bound clump, on a much longer timescale (10^2–10^3 orbits). *Cuzzi et al.* (2008) suggested a criterion for stability of these bound, yet only slowly shrinking, clumps that led directly to the conclusion that they would preferentially form large planetesimals comparable in size with the mass-dominant 100-km-radius mode advocated for the early asteroid belt by *Bottke et al.* (2005) — thus leaping over the long-troublesome millimeter- to meter- to kilometer-sized barriers. Objects formed in this way are compatible with the primary texture seen in the most primitive unbrecciated CM and CO chondrites (*Metzler et al.,* 1992; *Brearley,* 1993), and would display deep homogeneity of bulk chemical and isotopic properties.

Cuzzi et al. (2010) and *Chambers* (2010) went on to describe an end-to-end primary accretion scenario, combining stability thresholds with calculated probability distributions of clump density, finding that a range of nebula conditions (all implying >10× local enhancement of the usually assumed 1% cosmic solids-to-gas ratio within some few 10^4 km of the mid-plane) could match the required rate of planetesimal formation and the characteristic mass mode around 100–200-km diameter. *Cuzzi et al.* (2010) gave a number of caveats regarding the built-in assumptions of this model; one caveat regarding scale-dependence of the concentration process has been found to be important enough to change the predictions of the scenario quantitatively (see below). Subsequently, *Cuzzi and Hogan* (2012) resolved a discrepancy in a key timescale between *Cuzzi et al.* (2010) and *Chambers* (2010), which makes planetesimal formation 1000× faster than in *Cuzzi et al.* (2010) [and correspondingly slower than in *Chambers* (2010)].

5.2. New Insights into Turbulent Concentration

The primary issues are whether it is *always* Kolmogorov friction time particles that are most effectively concentrated, and whether the physics of their concentration are scale-invariant. *Hogan and Cuzzi* (2007) argued by analogy with the observed scale-invariance of turbulent dissipation, which is dominated by Kolmogorov-time vortex tubes (little tornados in turbulence) that the concentration of Kolmogorov-friction-time particles would also be scale-invariant (see also *Cuzzi and Hogan,* 2012). They developed a so-called cascade model by which to extend the low-Re results to nebula conditions.

The primary accretion scenarios of *Cuzzi et al.* (2010) and *Chambers* (2010) used this cascade model to generate density-vorticity probability density functions (PDFs) as a function of nebula scale. *Pan et al.* (2011) ran simulations at higher Re than *Hogan and Cuzzi* (2007) and found that the clump density PDFs dropped faster than would be predicted by the scale-invariant cascade. They suggested that the physics of particle concentration might indeed be scale-dependent, and that planetesimal formation rates obtained using the *Hogan and Cuzzi* (2007) cascade might be significantly overestimated.

Ongoing work supports this concern about scale dependence. *Cuzzi et al.* (2014) have analyzed much higher Re simulations (*Bec et al.,* 2010) and found that the cascade measures, called "multiplier distributions," that determine how strongly particles get clustered at each spatial scale *do* depend on scale at least over the largest decade or so of length scale; i.e., the scale-invariant inertial range for particle concentration and dissipation does not become established at the largest scale, causing little concentration to occur until roughly an order of magnitude smaller scale. Because the cascade process is multiplicative, this slow start means that fewer dense zones are to be found at any given scale size than previously thought.

New, scale-dependent cascades can now be implemented to predict planetesimal IMFs using the approach of *Cuzzi et al.* (2010, 2014). The quantitative implications are not clear as yet, but particles with friction times significantly longer than those of single chondrules are most strongly clustered at length scales most relevant to direct planetesimal formation (see also *Bec et al.,* 2007). Meanwhile, turbulent concentration of small particles may play a critical and as yet unmodeled (in astrophysics) role in formation of aggregates by collisions and sticking (see, e.g., *Shaw,* 2003; *Pan et al.,* 2011) (section 4). Some combination of these effects probably contributes to observed chondrule size distributions, some (but not all) of which appear broader than previously thought (*Fisher et al.,* 2014; *Friedrich et al.,* 2015; *Ebel et al.,* 2015).

6. PRESSURE BUMPS AND STREAMING INSTABILITY

The turbulent concentration mechanism described in the previous section operates on the smallest scales of the turbulent flow (although the vortical structures that expel particles can be very elongated). The dynamical timescales on such small-length scales are much shorter than the local orbital timescale of the protoplanetary disk. In contrast, the largest scales of the turbulent flow are dominated by the Coriolis force, and this allows for the emergence of large-scale geostrophic structures (high-pressure regions in perfect balance between the outward-directed pressure gradient force and the inward-directed Coriolis force).

Whipple (1972) found that particles are trapped by the zonal flow surrounding large-scale pressure bumps. Pressure bumps [in a way azimuthally extended analogs to the vortices envisioned in *Barge and Sommeria* (1995)] can arise through an inverse cascade of magnetic energy (*Johansen et al.,* 2009a; *Simon et al.,* 2012; *Dittrich et al.,* 2013) in tur-

bulence driven by the magnetorotational instability (*Balbus and Hawley,* 1991). Pressure bumps concentrate primarily large (0.1–10 m) particles that couple to the gas on an orbital timescale (*Johansen et al.,* 2006), reaching densities at least 100× the gas density, which leads to the formation of 1000-km-scale planetesimals (*Johansen et al.,* 2007, 2011). The magnetorotational instability is nevertheless no longer favored as the main driver of angular momentum transport in the asteroid-formation region of the solar protoplanetary disk, since the ionization degree is believed to be too low for coupling the gas to the magnetic field (see review by *Turner et al.,* 2014).

The magnetorotational instability can still drive turbulence (with α in the interval from 10^{-3} to 10^{-2}) in the mid-plane close to the star (within approximately 1 AU where the ionization is thermal) and far away from the star (beyond 20 AU where ionizing cosmic rays and X-rays penetrate to the mid-plane). Accretion through the "dead zone," situated between these regions of active turbulence, can occur in ionized surface layers far above the mid-plane (*Oishi et al.,* 2007), from disk winds (*Bai and Stone,* 2013) and by purely hydrodynamical instabilities in the vertical shear of the gas (*Nelson et al.,* 2013) or radial convection arising from the subcritical baroclinic instability (*Klahr and Bodenheimer,* 2003; *Lesur and Papaloizou,* 2010). The mid-plane is believed to be stirred to a mild degree by these hydrodynamical instabilities or by perturbations from the active layers several scale-heights above the mid-plane, driving effective turbulent diffusivities in the interval from 10^{-5} to 10^{-3} in the mid-plane. The inner and outer edges of this "dead zone," where the turbulent viscosity transitions abruptly, are also possible sites of pressure bumps and large-scale Rossby vortices that feed off the pressure bumps (*Lyra et al.,* 2008, 2009).

6.1. Streaming Instability

The low degree of turbulent stirring in the asteroid-formation region also facilitates the action of the streaming instability, a mechanism where particles take an active role in the concentration process (*Youdin and Goodman,* 2005; *Youdin and Johansen,* 2007; *Johansen and Youdin,* 2007). The instability arises from the speed difference between gas and solid particles. The gas is slightly pressure-supported in the direction pointing away from the star, due to the higher temperature and density close to the star, which mimics a reduced gravity on the gas. The result is that the gas orbital speed is approximately 50 m s^{-1} slower than the Keplerian speed at any given distance from the star. Solid particles are not affected by the global pressure gradient — they would move at the Keplerian speed in the absence of drag forces, but drift radially due to the friction from the slower-moving gas. The friction exerted from the particles back onto the gas leads to an instability whereby a small overdensity of particles accelerates the gas and diminishes the difference from the Keplerian speed. The speed increase in turn reduces the local headwind on the dust. This slows down the radial drift of particles locally, which leads to a runaway process where isolated particles drift into the convergence zone and the density increases exponentially with time. This picture is a bit simplified, as *Youdin and Goodman* (2005) and *Jacquet et al.* (2011) showed that the streaming instability operates only in the presence of rotation, i.e., the instability relies on the presence of Coriolis forces. This explains why the instability occurs on relatively large scales of the protoplanetary disk where Coriolis forces are important, typically a fraction of an astronomical unit, and operates most efficiently on large particles with frictional coupling times around one-tenth of the orbital timescale (typically decimeter sizes at the location of the asteroid belt).

6.2 Computer Simulations of the Streaming Instability

Computer simulations that follow the evolution of the streaming instability into its nonlinear regime show the emergence of axisymmetric filaments with typical separations of 0.2× the gas scale-height (*Yang and Johansen,* 2014) and local particle densities reaching several thousand times the gas density (*Bai and Stone,* 2010; *Johansen et al.,* 2012). These high densities trigger the formation of large planetesimals (100–1000 km in diameter) by gravitational fragmentation of the filaments (*Johansen et al.,* 2007), although planetesimal sizes decrease to approximately 100 km for a particle column density comparable to that of the solar protoplanetary disk (*Johansen et al.,* 2012).

An important question concerning planetesimal formation through the streaming instability is whether the process can operate for particles as small as chondrules in the asteroid belt. In Fig. 3, we show numerical experiments from *Carrera et al.* (2015) on the streaming instability in particles with sizes down to a fraction of a millimeter. The streaming instability requires a threshold particle mass loading $Z = \Sigma_p/\Sigma_g$, where Σ_p and Σ_g are the particle and gas column densities, to trigger the formation of overdense filaments (*Johansen et al.,* 2009b; *Bai and Stone,* 2010). The simulations in Fig. 3 start at $Z = Z_0 = 0.01$, but the particle mass-loading is continuously increased by removing the gas on a timescale of 30 orbital periods. This was done to identify how the critical value of Z depends on the particle size. The result is that overdense filaments form already at $Z = 0.015$ for centimeter-sized particles, while large chondrules of millimeter sizes require $Z = 0.04$ to trigger filament formation. Chondrules smaller than millimeters do not form filaments even at $Z = 0.08$.

A lowered gas column density may thus be required to trigger concentration of chondrule-sized particles by the streaming instability. It is possible that the solar protoplanetary disk had a lower gas density than what is inferred from the current mass of rock and ice in the planets (which multiplied by 100 gives the MMSN), if the planet-forming regions of the nebula were fed by pebbles drifting in from larger orbital distances (*Birnstiel et al.,* 2012). In this picture the growing planetesimals and planets are fed by drifting pebbles, so that the current mass of the planets was achieved by the integrated capture efficiency of the drifting solids; this

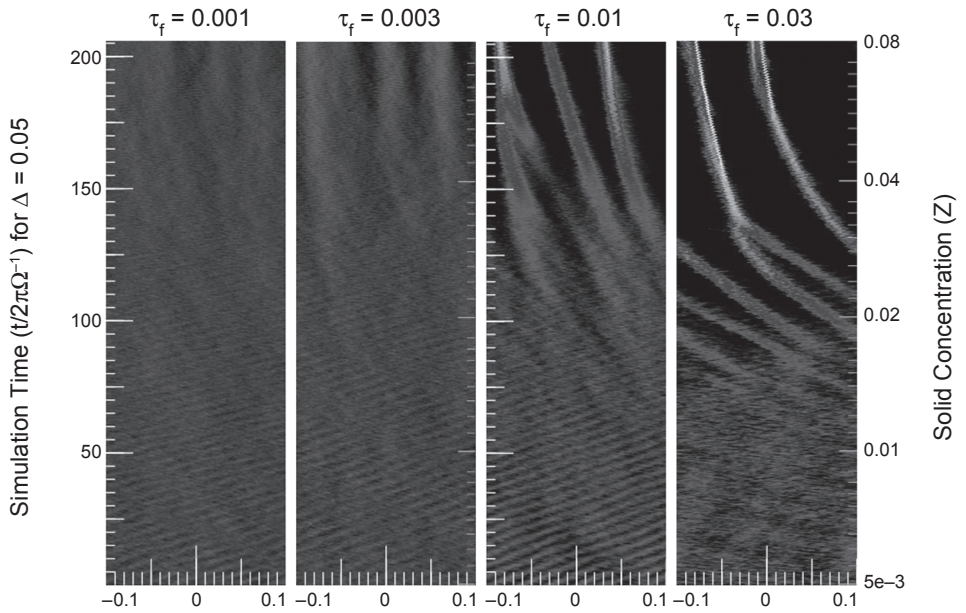

Fig. 3. Space-time plots of particle concentration by streaming instabilities, from *Carrera et al.* (2015), with the x-axis indicating the radial distance from the center of the simulation box and the y-axis the time (on the left) and the dust-to-gas ratio (on the right). The four columns show particle sizes 0.8 mm ($\tau_f = 0.001\Omega^{-1}$), 2.4 mm ($\tau_f = 0.003\Omega^{-1}$), 8 mm ($\tau_f = 0.01\Omega^{-1}$), and 2.4 cm ($\tau_f = 0.03\Omega^{-1}$). Simulations start with a mean dust-to-gas ratio of Z = 0.01, but gas is removed on a timescale of 30 orbits (1 orbit = $2\pi\Omega^{-1}$), increasing the dust-to-gas ratio accordingly . While centimeter-sized particles concentrate in overdense filaments already at a modest increase in dust-to-gas ratio to Z = 0.015, smaller particles require consecutively increasing gas removal to trigger clumping.

allows for gas column densities lower than in the MMSN to be consistent with the current masses of planets in the solar system. The gas will also be removed by accretion and photoevaporation (*Alexander and Armitage,* 2006). The high mass-loading in the gas could be obtained through pileup by radial drift and release of refractory grains near the iceline (*Sirono,* 2011).

Turbulence as weak as $\alpha \sim 10^{-7}$ is necessary to allow the sedimentation of chondrules (with $St \sim 10^{-3}$) into a thin mid-plane layer with scale-height $H_p = 0.01H_g$ and $\rho_p \approx \rho_g$ (see equation (2)), the latter being a necessary density criterion for activating particle pileup by streaming instabilities. Very low levels of α are consistent with protoplanetary disk models where angular momentum is transported by disk winds and the mid-plane remains laminar (*Bai and Stone,* 2013), except for mild stirring by Kelvin-Helmholtz (*Youdin and Shu,* 2002) and streaming instabilities (*Bai and Stone,* 2010).

Weak turbulence also facilitates the formation of decimeter-sized chondrule aggregates (*Ormel et al.,* 2008), which would concentrate much more readily in the gas. Stirring by hydrodynamical instabilities in the mid-plane, such as the vertical shear instability (*Nelson et al.,* 2013), would preclude significant sedimentation of chondrule-sized particles and affect the streaming instability, as well as the formation of chondrule aggregates, negatively. An alternative possibility is that the first asteroid seeds in fact did not form from chondrules (or chondrule aggregates), but rather from larger icy particles that would have been present in the asteroid-formation region in stages of the protoplanetary disk where the iceline was much closer to the star (*Martin and Livio,* 2012; *Ros and Johansen,* 2013). Chondrules could have been incorporated by later chondrule accretion (see section 7).

7. LAYERED ACCRETION

The turbulent concentration model and the streaming instability, reviewed in the previous sections, are the leading contenders for primary accretion of chondrules into chondrites. However, neither of the two are completely successful in explaining the dominance of chondrules in chondrites: The turbulent concentration models may not be able to concentrate sufficient amounts for gravitational collapse, while the streaming instability relies on the formation of chondrule aggregates and/or gas depletion and pileup of solid material from the outer parts of the protoplanetary disk. In the layered accretion model the chondrules are instead accreted onto the growing asteroids over millions of years after the formation of the first asteroid seeds — those first seeds forming by direct coagulation from a population of 100-m-sized planetesimals as envisioned in *Weidenschilling* (2011) or by one or more of the particle concentration mechanisms described in the previous sections.

7.1. Chondrule Accretion

Chondrules are perfectly sized for drag-force-assisted accretion onto young asteroids. The ubiquity of chondrules inside chondrites, and their large age spread (*Connelly et al.,* 2012), indicates that planetesimals formed and orbited within a sea of chondrules. Chondrules would have been swept past these young asteroids with the sub-Keplerian gas. The gas is slightly pressure-supported in the radial direction and hence moves slower than the Keplerian speed by the positive amount Δv (*Weidenschilling,* 1977b; *Nakagawa et al.,* 1986). The Bondi radius $R_B = GM/(\Delta v)^2$ marks the impact parameter for gravitational scattering of a chondrule by an asteroid of mass M, with

$$\frac{R_B}{R} = 0.87\left(\frac{R}{50\text{ km}}\right)^2\left(\frac{\Delta v}{53\text{ m s}^{-1}}\right)^{-2}\left(\frac{\rho_\bullet}{3.5\text{ g cm}^{-3}}\right) \quad (4)$$

Here we have normalized by $\Delta v = 53$ m s^{-1}, the nominal value in the MMSN model of *Hayashi* (1981), and used the chondrule density $\rho_\bullet = 3.5$ g cm^{-3} as a reference value. Chondrules with friction time comparable to the Bondi timescale $t_B = R_B/\Delta v$ are accreted by the asteroid (*Johansen and Lacerda,* 2010; *Ormel and Klahr,* 2010; *Lambrechts and Johansen,* 2012). The accretion radius R_{acc} can be calculated numerically as a function of asteroid size and chondrule size by integrating the trajectory of a chondrule moving with the sub-Keplerian gas flow past the asteroid. The accretion radius peaks at $R_{acc} \approx R_B$ for t_f/t_B in the range from 0.5 to 10 (*Lambrechts and Johansen,* 2012). Accretion at the full Bondi radius happens for particle sizes

$$a = [0.008, 0.16]\text{mm}\left(\frac{R}{50\text{ km}}\right)^3\left(\frac{\Delta v}{53\text{ m s}^{-1}}\right)^{-3} \times \left(\frac{r}{2.5\text{ AU}}\right)^{-3}\left(\frac{\Sigma_g}{\Sigma_{MMSN}}\right) \quad (5)$$

An asteroid of radius 50 km thus "prefers" to accrete chondrules of sizes smaller than 0.1 mm, corresponding to the smallest chondrules found in chondrites. At 100 km in radius, the preferred chondrule size is closer to 0.2 mm, a 200-km-radius body prefers millimeter-sized chondrules, and larger bodies can only grow efficiently if they can accrete chondrules of several millimeters or centimeters in diameter. Carbonaceous chondrites accreted significant amounts of CAIs and matrix together with their chondrules; *Rubin* (2011) suggested that matrix was accreted in the form of centimeter-sized porous aggregates with aerodynamical friction time comparable to chondrules and CAIs.

Aerodynamical accretion of chondrules could explain the narrow range of chondrule sizes found in the various classes of meteorites. The model predicts that asteroids accrete increasingly larger chondrules as they grow. This prediction may be at odds with the little variation in chondrule sizes found within chondrite classes [70% of EH3 and CO3 chondrules have apparent diameters within a factor of 2 of the mean apparent diameters in the group, according to *Rubin* (2000)]. The least-metamorphosed LL chondrites nevertheless do seem to host on the average larger chondrules (*Nelson and Rubin,* 2002). More metamorphosed LL chondrites actually show a lack of small chondrules; this could be due to the fact that the smallest chondrules disappeared from the strongly heated central regions of the parent body.

7.2 Chondrule Accretion Rates

The accretion rate of chondrules (and other macroscopic particles) is

$$\dot{M} = \pi f_B^2 R_B^2 \rho_p \Delta v \quad (6)$$

Here f_B parameterizes the actual accretion radius relative to the Bondi radius and ρ_p is the chondrule density. Accretion of chondrules is a runaway process, since $\dot{M} \propto R_B^2 \propto M^2$ if the optimal chondrule size is present (so that $f_B = 1$ in equation (6)). The characteristic growth timescale is

$$t_{exp} = \frac{M}{\dot{M}} = 1.66\text{ m.y.}\left(\frac{R}{50\text{ km}}\right)^{-3}\left(\frac{\Delta v}{53\text{ m s}^{-1}}\right)^3 \times \left(\frac{r}{2.5\text{ AU}}\right)^{2.75}\left(\frac{\Sigma_g}{\Sigma_{MMSN}}\right)^{-1}\left(\frac{\rho_\bullet}{3.5\text{ g cm}^{-3}}\right)^{-1} \quad (7)$$

We assumed here that the chondrules have sedimented to a thin mid-plane layer of thickness 1% relative to the gas scale-height. The strong dependence of the accretion rate on the planetesimal mass will drive a steep differential size distribution of a population of planetesimals accreting chondrules. This is illustrated in Fig. 4, where asteroid seeds with initial sizes from 10 to 50 km in radius have been exposed to chondrule accretion over 5 m.y. The value of the turbulent viscosity is $\alpha = 2 \times 10^{-6}$. The resulting differential size distribution (which manifests itself after around 3 m.y. of chondrule accretion) shows a bump at 70 km in radius, a steep decline toward 200 km in radius, and finally a slower decline toward larger asteroids. The shallower decline is caused by the lack of centimeter-sized particles needed to drive the continued runaway accretion of large asteroids (this can be seen as a drop in f_B in equation (6)). All the features in the size distribution in Fig. 4 are in good agreement with features of the observed size distribution of asteroids that are not explained well in coagulation models (*Morbidelli et al.,* 2009).

Layered accretion of chondrules can readily explain the large age spread of individual chondrules inside chondrites (*Connelly et al.,* 2012), as well as the remnant magnetization of the Allende meteorite (*Elkins-Tanton et al.,* 2011), imposed on the accreted chondrules from the internal dynamo in the

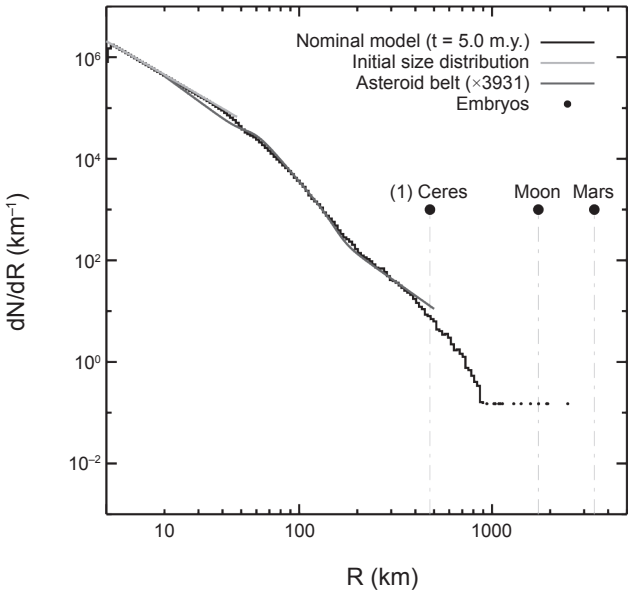

Fig. 4. The size distribution of asteroids and planetary embryos after accreting chondrules with sizes from 0.1 to 1.6 mm in diameter for 5 m.y. The original asteroid sizes had sizes between 10 and 50 km in radius (light gray line), here envisioned to form by the streaming instability in a population of decimeter-sized icy particles. The resulting size distribution of asteroids is in good agreement with the bump at 70 km in radius, the steep size distribution from 70 km to 200 km, and the shallower size distribution of larger asteroids whose chondrule accretion is slowed down by friction within their very large Bondi radius. Figure based on *Johansen et al.* (2015).

parent body's molten core. Efficient chondrule accretion requires, as does the streaming instability discussed in the previous section, sedimentation of chondrules to a thin mid-plane layer. The turbulent viscosity of $\alpha = 2 \times 10^{-6}$ in Fig. 4 is nevertheless significantly larger than the $\alpha \sim 10^{-7}$ needed to sediment chondrules to a thin mid-plane layer of thickness 1% of the gas scale height; indeed the timescale to grow to the current asteroid population is 3 m.y. in the simulation shown in Fig. 4, about twice as long as in equation (7), but in good agreement with the ages of the youngest chondrules.

8. OPEN QUESTIONS

The formation of asteroids is a complex problem that will only be solved through a collective effort from astronomers, planetary scientists, and cosmochemists. Although many details of asteroid formation are still not understood, we hope to have convinced the reader that new insights have been achieved in many areas in the past years. Here we highlight 10 areas of open questions in which we believe that major progress will be made in the next decade:

1. *Short-lived radionuclides.* What is the origin of the short-lived radioactive elements that melted the differentiated parent bodies? Was ^{26}Al heterogeneous in the solar protoplanetary disk? How did the young solar system become polluted in ^{26}Al without receiving large amounts of ^{60}Fe, an element that is copiously produced in supernovae?

2. *Maintaining free-floating chondrules and CAIs.* How is it possible to preserve chondrules and CAIs for millions of years in the disk before storing them in a chondritic body, without mixing them too much to erase chondrule classes and chondrule-matrix complementarity? What are we missing that makes this issue so paradoxical?

3. *Chondrules vs. matrix.* Why do carbonaceous chondrites contain large amounts of matrix while ordinary chondrites contain very little matrix? Did the matrix enter the chondrites as (potentially icy) "matrix lumps" or on fine-grained rims attached to chondrules and other macroscopic particles?

4. *Initial asteroid sizes.* What is the origin of the steep differential size distribution of asteroids beyond the knee at 100 km? Did asteroids form small as in the coagulation picture, medium-sized as in the layered accretion model, or large as in some turbulent concentration models? Why do Kuiper belt objects, which formed under very different conditions in temperature and density, display a similar size distribution as asteroids?

5. *The origin of asteroid classes.* How is the radial gradient of asteroid composition produced and retained in the presence of considerable preaccretionary turbulent mixing and postaccretionary dynamical mixing? Is asteroid formation a continuous process that happens throughout the lifetime of the protoplanetary disk? What do the different chondrite groups mean in terms of formation location and time?

6. *Dry and wet chondrites.* Why do we have dry chondrites (enstatite, ordinary)? If chondrites form at 2–4 m.y. after CAIs, then the snowline should have been well inside the inner edge of the asteroid belt. Are there overlooked heating sources that could keep the iceline at 3 AU throughout the lifetime of the protoplanetary disk? Or did the asteroid classes form at totally different places only to be transported to their current orbits later?

7. *Internal structure of asteroids.* Does the chondrite and asteroid family evidence suggest that the primary asteroids — before internal heating — are homogeneous, roughly 100-km-diameter bodies composed of a physically, chemically, and isotopically homogeneous mix of chondrule-sized components? Or is internal heterogeneity, as may be the case for the Allende parent body, prevalent?

8. *Turbulent concentration of chondrules.* Under what nebula conditions can vortex tubes over a range of nebula scales concentrate enough chondrules into volumes that are gravitationally bound, at a high enough rate to produce the primordial asteroids and meteorite parent bodies directly? What other roles could turbulent concentration play in planetesimal formation given that the optimally concentrated particle is chondrule-sized under nominal values of the turbulent viscosity?

9. *Streaming instability with chondrules.* Will the conditions for streaming instabilities to concentrate chondrule-sized particles, i.e., gas depletion and/or particle pileup, be fulfilled in the protoplanetary disk? How does an overdense

filament of chondrule-sized particles collapse under self-gravity given the strong support by gas pressure?

10. *Layered accretion.* What is the origin of the apparent scarcity of heterogeneous asteroid families, given that asteroids orbiting within an ocean of chondrules should accrete these prodigiously? What is the thermal evolution of early-formed asteroid seeds that continue to accrete chondrules over millions of years?

Acknowledgments. A.J. was supported by the Swedish Research Council (grant 2010-3710), the European Research Council under ERC Starting Grant agreement 278675-PEBBLE2PLANET, and the Knut and Alice Wallenberg Foundation. He would like to thank B. Weiss for stimulating discussions on layered accretion. E.J. wishes to remember his colleague and friend G. Barlet (1985–2014), who as a short-lived radionuclide theorist and chondrule/refractory inclusion specialist would certainly have contributed to the new paradigms discussed herein, true to his attachment to interdisciplinary interactions, but left us far too early. J.C. thanks C. Ormel for a careful reading, and E. Scott, A. Rubin, N. Kita, and G. Wasserburg for helpful comments and references. We would like to thank A. Rubin and an additional anonymous referee for insightful referee reports.

REFERENCES

Alexander C. M. O. and Ebel D. S. (2012) Questions, questions: Can the contradictions between the petrologic, isotopic, thermodynamic, and astrophysical constraints on chondrule formation be resolved? *Meteoritics & Planet. Sci., 47,* 1157.

Alexander C. M. O., Grossman J. N., Ebel D. S., et al. (2008) The formation conditions of chondrules and chondrites. *Science, 320,* 1617.

Alexander R. D. and Armitage P. J. (2006) The stellar mass-accretion rate relation in T Tauri stars and brown dwarfs. *Astrophys. J. Lett., 639,* L83.

Arnould M., Paulus G., and Meynet G. (1997) Short-lived radionuclide production by non-exploding Wolf-Rayet stars. *Astron. Astrophys., 321,* 452.

Bai X.-N. and Stone J. M. (2010) Dynamics of solids in the midplane of protoplanetary disks: Implications for planetesimal formation. *Astrophys. J., 722,* 1437.

Bai X.-N. and Stone J. M. (2013) Wind-driven accretion in protoplanetary disks. I. Suppression of the magnetorotational instability and launching of the magnetocentrifugal wind. *Astrophys. J., 769,* 76.

Balbus S. A. and Hawley J. F. (1991) A powerful local shear instability in weakly magnetized disks. I — Linear analysis. II — Nonlinear evolution. *Astrophys. J., 376,* 214.

Barge P. and Sommeria J. (1995) Did planet formation begin inside persistent gaseous vortices? *Astron. Astrophys., 295,* L1.

Bec J., Biferale L., Cencini M., et al. (2007) Heavy particle concentration in turbulence at dissipative and inertial scales. *Phys. Rev. Lett., 98(8),* Article ID 084502.

Bec J., Biferale L., Cencini M., et al. (2010) Intermittency in the velocity distribution of heavy particles in turbulence. *J. Fluid Mech., 646,* 527.

Beckwith S. V. W., Henning T., and Nakagawa Y. (2000) Dust properties and assembly of large particles in protoplanetary disks. In *Protostars and Planets IV* (V. Mannings et al., eds.), p. 533. Univ. of Arizona, Tucson.

Beitz E., Güttler C., Blum J., et al. (2011) Low-velocity collisions of centimeter-sized dust aggregates. *Astrophys. J., 736,* 34.

Birnstiel T., Dullemond C. P., and Brauer F. (2010) Gas- and dust evolution in protoplanetary disks. *Astron. Astrophys., 513,* A79.

Birnstiel T., Ormel C. W., and Dullemond C. P. (2011) Dust size distributions in coagulation/fragmentation equilibrium: Numerical solutions and analytical fits. *Astron. Astrophys., 525,* A11.

Birnstiel T., Klahr H., and Ercolano B. (2012) A simple model for the evolution of the dust population in protoplanetary disks. *Astron. Astrophys., 539,* A148.

Bitsch B., Morbidelli A., Lega E., et al. (2014) Stellar irradiated discs and implications on migration of embedded planets. III. Viscosity transitions. *Astron. Astrophys., 570,* A75.

Bitsch B., Johansen A., Lambrechts L., and Morbidelli A. (2015) The structure of protoplanetary discs around evolving young stars. *Astron. Astrophys., 575,* A28.

Bland P. A., Howard L. E., Prior D. J., et al. (2011) Earliest rock fabric formed in the solar system preserved in a chondrule rim. *Nature Geosci., 4,* 244.

Blum J. and Wurm G. (2008) The growth mechanisms of macroscopic bodies in protoplanetary disks. *Annu. Rev. Astron. Astrophys., 46,* 21.

Boss A. P. (1996) A concise guide to chondrule formation models. In *Chondrules and the Protoplanetary Disk* (R. H. Hewins et al., eds.) pp. 257–263. Cambridge Univ., Cambridge.

Boss A. P. and Keiser S. A. (2013) Triggering collapse of the presolar dense cloud core and injecting short-lived radioisotopes with a shock wave. II. Varied shock wave and cloud core parameters. *Astrophys. J., 770,* 51.

Bottke W. F., Durda D. D., Nesvorný D., et al. (2005) The fossilized size distribution of the main asteroid belt. *Icarus, 175,* 111.

Bottke W. F., Vokrouhlický D., Minton D., et al. (2012) An Archaean heavy bombardment from a destabilized extension of the asteroid belt. *Nature, 485,* 78.

Brauer F., Dullemond C. P., and Henning T. (2008) Coagulation, fragmentation and radial motion of solid particles in protoplanetary disks. *Astron. Astrophys., 480,* 859.

Brearley A. J. (1993) Matrix and fine-grained rims in the unequilibrated CO3 chondrite, ALHA77307 — Origins and evidence for diverse, primitive nebular dust components. *Geochim. Cosmochim. Acta, 57,* 1521.

Brearley A. J. (1996) Nature of matrix in unequilibrated chondrites and its possible relationship to chondrules. In *Chondrules and the Protoplanetary Disk* (by R. H. Hewins et al., eds.), pp. 137–151. Cambridge Univ., Cambridge.

Brearley A. J. (2003) Nebular versus parent-body processing. In *Treatise on Geochemistry, Vol. 1: Meteorites, Comets and Planets* (A. M. Davis, ed.), p. 247. Elsevier, Amsterdam.

Brearley A. and Jones A. (1998) Chondritic meteorites. In *Planetary Materials* (J. J. Papike, ed.), pp. 3-1 to 3-398. Mineralogical Society of America, Chantilly, Virginia.

Burbine T. H., McCoy T. J., Meibom A., et al. (2002) Meteoritic parent bodies: Their number and identification. In *Asteroids III* (W. F. Bottke Jr. et al., eds.), pp. 653–667. Univ. of Arizona, Tucson.

Cameron A. G. W. and Truran J. W. (1977) The supernova trigger for formation of the solar system. *Icarus, 30,* 447.

Carrera D., Johansen A., and Davies M. B. (2015) Formation of asteroids from mm-sized chondrules. *Astron. Astrophys., 579,* A43.

Chambers J. E. (2010) Planetesimal formation by turbulent concentration. *Icarus, 208,* 505.

Chaussidon M. and Barrat J.-A. (2009) ^{60}Fe in eucrite NWA 4523: Evidences for secondary redistribution of Ni and for secondary apparent high ^{60}Fe/^{56}Fe ratios in troilite. *Lunar Planet. Sci. XL,* Abstract #1752. Lunar and Planetary Institute, Houston.

Chen J. H., Papanastassiou D. A., Telus M., et al. (2013) Fe-Ni isotopic systematics in UOC QUE 97008 and Semarkona chondrules. *Lunar Planet. Sci. XLIV,* Abstract #2649. Lunar and Planetary Institute, Houston.

Chevalier R. A. (1999) Supernova remnants in molecular clouds. *Astrophys. J., 511,* 798.

Chevalier R. A. (2000) Young circumstellar disks near evolved massive stars and supernovae. *Astrophys. J. Lett., 538,* L151.

Chiang E. and Youdin A. N. (2010) Forming planetesimals in solar and extrasolar nebulae. *Annu. Rev. Earth Planet. Sci., 38,* 493.

Ciesla F. J., Lauretta D. S., and Hood L. L. (2004) The frequency of compound chondrules and implications for chondrule formation. *Meteoritics & Planet. Sci., 39,* 531.

Clayton R. N., Mayeda T. K., Olsen E. J., et al. (1991) Oxygen isotope studies of ordinary chondrites. *Geochim. Cosmochim. Acta, 55,* 2317.

Connolly H. C. Jr. and Desch S. J. (2004) On the origin of the "kleine Kugelchen" called chondrules. *Chem. Erde–Geochem., 64,* 95.

Connelly J. N., Bizzarro M., Krot A. N., et al. (2012) The absolute chronology and thermal processing of solids in the solar protoplanetary disk. *Science, 338,* 651.

Cuzzi J. N. (2004) Blowing in the wind: III. Accretion of dust rims by chondrule-sized particles in a turbulent protoplanetary nebula. *Icarus, 168,* 484.

Cuzzi J. N. and Alexander C. M. O. (2006) Chondrule formation in particle-rich nebular regions at least hundreds of kilometers across. *Nature, 441,* 483.

Cuzzi J. N. and Hogan R. C. (2003) Blowing in the wind. I. Velocities of chondrule-sized particles in a turbulent protoplanetary nebula. *Icarus, 164,* 127.

Cuzzi J. N. and Hogan R. C. (2012) Primary accretion by turbulent concentration: The rate of planetesimal formation and the role of vortex tubes. *Lunar Planet. Sci. XLIII,* Abstract #2536. Lunar and Planetary Institute, Houston.

Cuzzi J. N. and Weidenschilling S. J. (2006) Particle-gas dynamics and primary accretion. In *Meteorites and the Early Solar System II* (D. S. Lauretta and H. Y. McSween Jr., eds.), pp. 353–381. Univ. of Arizona, Tucson.

Cuzzi J. N., Dobrovolskis A. R., and Hogan R. C. (1996) Turbulence, chondrules, and planetesimals. In *Chondrules and the Protoplanetary Disk* (R. H. Hewins et al., eds.), pp. 35–43. Cambridge Univ., Cambridge.

Cuzzi J. N., Hogan R. C., Paque J. M., et al. (2001) Size-selective concentration of chondrules and other small particles in protoplanetary nebula turbulence. *Astrophys. J., 546,* 496.

Cuzzi J. N., Ciesla F. J., Petaev M. I., et al. (2005) Nebula evolution of thermally processed solids: Reconciling models and meteorites. In *Chondrites and the Protoplanetary Disk* (A. N. Krot et al., eds.), p. 732. ASP Conf. Series 341, Astronomical Society of the Pacific, San Francisco.

Cuzzi J. N., Hogan R. C., and Shariff K. (2008) Toward planetesimals: Dense chondrule clumps in the protoplanetary nebula. *Astrophys. J., 687,* 1432.

Cuzzi J. N., Hogan R. C., and Bottke W. F. (2010) Towards initial mass functions for asteroids and Kuiper Belt Objects. *Icarus, 208,* 518.

Cuzzi J. N., Hartlep T., Weston B., et al. (2014) Turbulent concentration of mm-size particles in the protoplanetary nebula: Scale-dependent multiplier functions. *Lunar Planet. Sci. XLIV,* Abstract #2764. Lunar and Planetary Institute, Houston.

Dauphas N. and Chaussidon M. (2011) A perspective from extinct radionuclides on a young stellar object: The Sun and its accretion disk. *Annu. Rev. Earth Planet. Sci., 39,* 351.

Deharveng L., Schuller F., Anderson L. D., et al. (2010) A gallery of bubbles. The nature of the bubbles observed by Spitzer and what ATLASGAL tells us about the surrounding neutral material. *Astron. Astrophys., 523,* A6.

Desch S. J., Morris M. A., Connolly H. C., et al. (2012) The importance of experiments: Constraints on chondrule formation models. *Meteoritics & Planet. Sci., 47,* 1139.

Dittrich K., Klahr H., and Johansen A. (2013) Gravoturbulent planetesimal formation: The positive effect of long-lived zonal flows. *Astrophys. J., 763,* 117.

Dodd R. T. (1976) Accretion of the ordinary chondrites. *Earth Planet. Sci. Lett., 30,* 281.

Dominik C. and Tielens A. G. G. M. (1997) The physics of dust coagulation and the structure of dust aggregates in space. *Astrophys. J., 480,* 647.

Dominik C., Blum J., Cuzzi J. N., et al. (2007) Growth of dust as the initial step toward planet formation. In *Protostars and Planets V* (B. Reipurth et al., eds.), pp. 783–800. Univ. of Arizona, Tucson.

Doyle P. M., Krot A. N., Nagashima K., et al. (2014) Manganese-chromium ages of aqueous alteration of unequilibrated ordinary chondrites. *Lunar Planet. Sci. XLIV,* Abstract #1726. Lunar and Planetary Institute, Houston.

Drążkowska J., Windmark F., and Dullemond C. P. (2013) Planetesimal formation via sweep-up growth at the inner edge of dead zones. *Astron. Astrophys., 556,* A37.

Eaton J. K. and Fessler J. R. (1994) Preferential concentration of particles by turbulence. *Intl. J. Multiphase Flow, Suppl., 20,* 169–209.

Ebel D., Brunner C., Leftwich K., Erb I., Lu M., Konrad K., Rodriguez H., Friedrich J., and Weisberg M. (2015) Abundance, composition and size of inclusions and matrix in CV and CO chondrites. *Geochim. Cosmochim. Acta,* in press.

Elkins-Tanton L. T., Weiss B. P., and Zuber M. T. (2011) Chondrites as samples of differentiated planetesimals. *Earth Planet. Sci. Lett., 305,* 1.

Eugster O., Herzog G. F., Marti K., et al. (2006) Irradiation records, cosmic-ray exposure ages, and transfer times of meteorites. In *Meteorites and the Early Solar System II* (D. S. Lauretta and H. Y. McSween Jr., eds.), pp. 829–851. Univ. of Arizona, Tucson.

Fisher K. R., Tait A. W., Simon J. I., et al. (2014) Contrasting size distributions of chondrules and inclusions in Allende CV3. *Lunar Planet. Sci. XLIV,* Abstract #2711. Lunar and Planetary Institute, Houston.

Fraser W. C., Brown M. E., Morbidelli A., et al. (2014) The absolute magnitude distribution of Kuiper belt objects. *Astrophys. J., 782,* 100.

Fressin F., Torres G., Charbonneau D., et al. (2013) The false positive rate of Kepler and the occurrence of planets. *Astrophys. J., 766,* 81.

Friedrich J. M., Weisberg M. K., Ebel D. S., Biltz A. E., Corbett B. M., Iotzov I. V., Khan W. S., and Wolman M. D. (2015) Chondrule size and related physical properties: A compilation and evaluation of current data across all meteorite groups. *Chem. Erde,* in press, DOI: 10.1016/j.chemer.2014.08.003.

Fu R. R. and Elkins-Tanton L. T. (2014) The fate of magmas in planetesimals and the retention of primitive chondritic crusts. *Earth Planet. Sci. Lett., 390,* 128.

Fujiya W., Sugiura N., Sano Y., et al. (2013) Mn-Cr ages of dolomites in CI chondrites and the Tagish Lake ungrouped carbonaceous chondrite. *Earth Planet. Sci. Lett., 362,* 130.

Gaidos E., Krot A. N., Williams J. P., et al. (2009) ^{26}Al and the formation of the solar system from a molecular cloud contaminated by Wolf-Rayet winds. *Astrophys. J., 696,* 1854.

Gail H.-P., Trieloff M., Breuer D., et al. (2014) Early thermal evolution of planetesimals and its impact on processing and dating of meteoritic material. In *Protostars and Planets VI* (H. Beuther et al., eds.), pp. 571–593. Univ. of Arizona, Tucson.

Gal-Yam A., Arcavi I., Ofek E. O., et al. (2014) AWolf-Rayet-like progenitor of SN 2013cu from spectral observations of a stellar wind. *Nature, 509,* 471.

Garaud P., Meru F., Galvagni M., et al. (2013) From dust to planetesimals: An improved model for collisional growth in protoplanetary disks. *Astrophys. J., 764,* 146.

Gounelle M. (2014) Aluminium-26 in the early solar system: A probability estimate. *Lunar Planet. Sci. XLIV,* Abstract #2113. Lunar and Planetary Institute, Houston.

Gounelle M. and Meibom A. (2008) The origin of short-lived radionuclides and the astrophysical environment of solar system formation. *Astrophys. J., 680,* 781.

Gounelle M. and Meynet G. (2012) Solar system genealogy revealed by extinct short-lived radionuclides in meteorites. *Astron. Astrophys., 545,* A4.

Gounelle M., Shu F. H., Shang H., et al. (2006) The irradiation origin of beryllium radioisotopes and other short-lived radionuclides. *Astrophys. J., 640,* 1163.

Gounelle M., Meibom A., Hennebelle P., et al. (2009) Supernova propagation and cloud enrichment: A new model for the origin of ^{60}Fe in the early solar system. *Astrophys. J. Lett., 694,* L1.

Gounelle M., Chaussidon M., and Rollion-Bard C. (2013) Variable and extreme irradiation conditions in the early solar system inferred from the initial abundance of ^{10}Be in Isheyevo CAIs. *Astrophys. J. Lett., 763,* L33.

Grimm R. E. and McSween H. Y. (1993) Heliocentric zoning of the asteroid belt by aluminum-26 heating. *Science, 259,* 653.

Guan Y., Huss G. R., Leshin L. A., et al. (2006) Oxygen isotope and ^{26}Al-^{26}Mg systematics of aluminum-rich chondrules from unequilibrated enstatite chondrites. *Meteoritics & Planet. Sci., 41,* 33.

Güttler C., Blum J., Zsom A., et al. (2010) The outcome of protoplanetary dust growth: Pebbles, boulders, or planetesimals? I. Mapping the zoo of laboratory collision experiments. *Astron. Astrophys., 513,* A56.

Hartmann L., Calvet N., Gullbring E., et al. (1998) Accretion and the evolution of T Tauri disks. *Astrophys. J., 495,* 385.

Hayashi C. (1981) Structure of the solar nebula, growth and decay of magnetic fields and effects of magnetic and turbulent viscosities on the nebula. *Progr. Theor. Phys. Suppl., 70,* 35.

Henke S., Gail H.-P., Trieloff M., et al. (2013) Thermal evolution model for the H chondrite asteroid-instantaneous formation versus protracted accretion. *Icarus, 226,* 212.

Hester J. J., Desch S. J., Healy K. R., et al. (2004) The cradle of the solar system. *Science, 304,* 1116.

Hewins R. H., Connolly H. C., Lofgren G. E., et al. (2005) Experimental constraints on chondrule formation. In *Chondrites and the Protoplanetary Disk* (A. N. Krot et al, eds.), pp. 286–316. ASP Conf. Series 341, Astronomical Society of the Pacific, San Francisco.

Hezel D. C. and Palme H. (2010) The chemical relationship between chondrules and matrix and the chondrule matrix complementarity. *Earth Planet. Sci. Lett., 294,* 85.
Hezel D. C., Russell S. S., Ross A. J., et al. (2008) Modal abundances of CAIs: Implications for bulk chondrite element abundances and fractionations. *Meteoritics & Planet. Sci., 43,* 1879.
Hogan R. C. and Cuzzi J. N. (2007) Cascade model for particle concentration and enstrophy in fully developed turbulence with mass-loading feedback. *Phys. Rev. E, 75(5),* Article ID 056305.
Huss G. R., Rubin A. E., and Grossman J. N. (2006) Thermal metamorphism in chondrites. In *Meteorites and the Early Solar System II* (D. S. Lauretta and H. Y. McSween Jr., eds.), pp. 567–586. Univ. of Arizona, Tucson.
Huss G. R., Meyer B. S., Srinivasan G., et al. (2009) Stellar sources of the short-lived radionuclides in the early solar system. *Geochim. Cosmochim. Acta, 73,* 4922.
Ida S., Guillot T., and Morbidelli A. (2008) Accretion and destruction of planetesimals in turbulent disks. *Astrophys. J., 686,* 1292.
Jacobsen B., Yin Q.-z., Moynier F., et al. (2008) ^{26}Al-^{26}Mg and ^{207}Pb-^{206}Pb systematics of Allende CAIs: Canonical solar initial ^{26}Al/^{27}Al ratio reinstated. *Earth Planet. Sci. Lett., 272,* 353.
Jacquet E. (2014a) The quasi-universality of chondrule size as a constraint for chondrule formation models. *Icarus, 232,* 176.
Jacquet E. (2014b) Transport of solids in protoplanetary disks: Comparing meteorites and astrophysical models. *Compt. Rend. Geosci., 346,* 3.
Jacquet E., Balbus S., and Latter H. (2011) On linear dust-gas streaming instabilities in protoplanetary discs. *Mon. Not. R. Astron. Soc., 415,* 3591.
Jacquet E., Alard O., and Gounelle M. (2012a) Chondrule trace element geochemistry at the mineral scale. *Meteoritics & Planet. Sci., 47,* 1695.
Jacquet E., Gounelle M., and Fromang S. (2012b) On the aerodynamic redistribution of chondrite components in protoplanetary disks. *Icarus, 220,* 162.
Jarosewich E. (1990) Chemical analyses of meteorites — A compilation of stony and iron meteorite analyses. *Meteoritics, 25,* 323.
Johansen A. and Lacerda P. (2010) Prograde rotation of protoplanets by accretion of pebbles in a gaseous environment. *Mon. Not. R. Astron. Soc., 404,* 475.
Johansen A. and Youdin A. (2007) Protoplanetary disk turbulence driven by the streaming instability: Nonlinear saturation and particle concentration. *Astrophys. J., 662,* 627.
Johansen A., Klahr H., and Henning T. (2006) Gravoturbulent formation of planetesimals. *Astrophys. J., 636,* 1121.
Johansen A., Oishi J. S., Mac Low M.-M., et al. (2007) Rapid planetesimal formation in turbulent circumstellar disks. *Nature, 448,* 1022.
Johansen A., Brauer F., Dullemond C., et al. (2008) A coagulation fragmentation model for the turbulent growth and destruction of preplanetesimals. *Astron. Astrophys., 486,* 597.
Johansen A., Youdin A., and Klahr H. (2009a) Zonal flows and long-lived axisymmetric pressure bumps in magnetorotational turbulence. *Astrophys. J., 697,* 1269.
Johansen A., Youdin A., and Mac Low M.-M. (2009b) Particle clumping and planetesimal formation depend strongly on metallicity. *Astrophys. J. Lett., 704,* L75.
Johansen A., Klahr H., and Henning T. (2011) High-resolution simulations of planetesimal formation in turbulent protoplanetary discs. *Astron. Astrophys., 529,* A62.
Johansen A., Youdin A. N., and Lithwick Y. (2012) Adding particle collisions to the formation of asteroids and Kuiper belt objects via streaming instabilities. *Astron. Astrophys., 537,* A125.
Johansen A., Blum J., Tanaka H., et al. (2014) The multifaceted planetesimal formation process. In *Protostars and Planets V* (B. Reipurth et al., eds.), pp. 547–570. Univ. of Arizona, Tucson.
Johansen A., Mac Low M.-M., Lacerda P., and Bizzarro M. (2015) Growth of asteroids, planetary embryos, and Kuiper belt objects by chondrule accretion. *Sci. Adv., 1(3),* 1500109.
Jones R. H. (2012) Petrographic constraints on the diversity of chondrule reservoirs in the protoplanetary disk. *Meteoritics & Planet. Sci., 47,* 1176.
Kastner J. H. and Myers P. C. (1994) An observational estimate of the probability of encounters between mass-losing evolved stars and molecular clouds. *Astrophys. J., 421,* 605.
Kato M. T., Fujimoto M., and Ida S. (2012) Planetesimal formation at the boundary between steady super/sub-Keplerian flow created by inhomogeneous growth of magnetorotational instability. *Astrophys. J., 747,* 11.
Keil K., Stoeffler D., Love S. G., et al. (1997) Constraints on the role of impact heating and melting in asteroids. *Meteoritics & Planet. Sci., 32,* 349.
Kita N. T. and Ushikubo T. (2012) Evolution of protoplanetary disk inferred from ^{26}Al chronology of individual chondrules. *Meteoritics & Planet. Sci., 47,* 1108.
Kita N. T., Yin Q.-Z., MacPherson G. J., et al. (2013) ^{26}Al-^{26}Mg isotope systematics of the first solids in the early solar system. *Meteoritics & Planet. Sci., 48,* 1383.
Klahr H. H. and Bodenheimer P. (2003) Turbulence in accretion disks: Vorticity generation and angular momentum transport via the global baroclinic instability. *Astrophys. J., 582,* 869.
Kretke K. A. and Lin D. N. C. (2007) Grain retention and formation of planetesimals near the snow line in MRI-driven turbulent protoplanetary disks. *Astrophys. J. Lett., 664,* L55.
Krot A., Petaev M., Russell S. S., et al. (2004) Amoeboid olivine aggregates and related objects in carbonaceous chondrites: Records of nebular and asteroid processes. *Chem. Erde–Geochem., 64,* 185.
Krot A. N., Amelin Y., Bland P., et al. (2009) Origin and chronology of chondritic components: A review. *Geochim. Cosmochim. Acta, 73,* 4963.
Kruijer T. S., Sprung P., Kleine T., et al. (2012) Hf-W chronometry of core formation in planetesimals inferred from weakly irradiated iron meteorites. *Geochim. Cosmochim. Acta, 99,* 287.
Kuebler K. E., McSween H. Y., Carlson W. D., et al. (1999) Sizes and masses of chondrules and metal-troilite grains in ordinary chondrites: Possible implications for nebular sorting. *Icarus, 141,* 96.
Lambrechts M. and Johansen A. (2012) Rapid growth of gas-giant cores by pebble accretion. *Astron. Astrophys., 544,* A32.
Lambrechts M., Johansen A., and Morbidelli A. (2014) Separating gas-giant and ice-giant planets by halting pebble accretion. *Astron. Astrophys., 572,* A35.
Larsen K. K., Trinquier A., Paton C., et al. (2011) Evidence for magnesium isotope heterogeneity in the solar protoplanetary disk. *Astrophys. J. Lett., 735,* L37.
Laughlin G., Steinacker A., and Adams F. C. (2004) Type I planetary migration with MHD turbulence. *Astrophys. J., 608,* 489.
Lauretta D. S., Nagahara H., and Alexander C. M. O. (2006) Petrology and origin of ferromagnesian silicate chondrules. In *Meteorites and the Early Solar System II* (D. S. Lauretta and H. Y. McSween, Jr., eds.), pp. 431–459. Univ. of Arizona, Tucson.
Lee T. (1978) A local proton irradiation model for isotopic anomalies in the solar system. *Astrophys. J., 224,* 217.
Lee T., Papanastassiou D. A., and Wasserburg G. J. (1976) Demonstration of Mg-26 excess in Allende and evidence for Al-26. *Geophys. Res. Lett., 3,* 41.
Lee T., Shu F. H., Shang H., et al. (1998) Protostellar cosmic rays and extinct radioactivities in meteorites. *Astrophys. J., 506,* 898.
Lesur G. and Papaloizou J. C. B. (2010) The subcritical baroclinic instability in local accretion disc models. *Astron. Astrophys., 513,* A60.
Libourel G. and Krot A. N. (2007) Evidence for the presence of planetesimal material among the precursors of magnesian chondrules of nebular origin. *Earth Planet. Sci. Lett., 254,* 1.
Liu M.-C., Chaussidon M., Göpel C., et al. (2012) A heterogeneous solar nebula as sampled by CM hibonite grains. *Earth Planet. Sci. Lett., 327,* 75.
Looney L. W., Tobin J. J., and Fields B. D. (2006) Radioactive probes of the supernova-contaminated solar nebula: Evidence that the Sun was born in a cluster. *Astrophys. J., 652,* 1755.
Lugaro M., Doherty C. L., Karakas A. I., et al. (2012) Short-lived radioactivity in the early solar system: The super-AGB star hypothesis. *Meteoritics & Planet. Sci., 47,* 1998.
Lyra W., Johansen A., Klahr H., et al. (2008) Embryos grown in the dead zone. Assembling the first protoplanetary cores in low mass self-gravitating circumstellar disks of gas and solids. *Astron. Astrophys., 491,* L41.
Lyra W., Johansen A., Zsom A., et al. (2009) Planet formation bursts at the borders of the dead zone in 2D numerical simulations of circumstellar disks. *Astron. Astrophys., 497,* 869.
MacPherson G. J. (2005) Calcium-aluminum-rich inclusions in chondritic meteorites. In *Treatise on Geochemistry, Vol. 1: Meteorites, Comets and Planets* (A. M. Davis, ed.), pp. 201–246. Elsevier, Amsterdam.

MacPherson G. J., Hashimoto A., and Grossman L. (1985) Accretionary rims on inclusions in the Allende meteorite. *Geochim. Cosmochim. Acta, 49,* 2267.
MacPherson G. J., Davis A. M., and Zinner E. K. (2014) Distribution of ^{26}Al in the early solar system: A 2014 reappraisal. *Lunar Planet. Sci. XLIV,* Abstract #2134. Lunar and Planetary Institute, Houston.
Makide K., Nagashima K., Krot A. N., et al. (2013) Heterogeneous distribution of ^{26}Al at the birth of the solar system: Evidence from corundum-bearing refractory inclusions in carbonaceous chondrites. *Geochim. Cosmochim. Acta, 110,* 190.
Martin R. G. and Livio M. (2012) On the evolution of the snow line in protoplanetary discs. *Mon. Not. R. Astron. Soc., 425,* L6.
Martin R. G. and Livio M. (2013) On the evolution of the snow line in protoplanetary discs — II. Analytic approximations. *Mon. Not. R. Astron. Soc., 434,* 633.
Metzler K. (2012) Ultrarapid chondrite formation by hot chondrule accretion? Evidence from unequilibrated ordinary chondrites. *Meteoritics & Planet. Sci., 47,* 2193.
Metzler K., Bischoff A., and Stoeffler D. (1992) Accretionary dust mantles in CM chondrites — Evidence for solar nebula processes. *Geochim. Cosmochim. Acta, 56,* 2873.
Mizuno H., Markiewicz W. J., and Voelk H. J. (1988) Grain growth in turbulent protoplanetary accretion disks. *Astron. Astrophys., 195,* 183.
Monnereau M., Toplis M. J., Baratoux D., et al. (2013) Thermal history of the H-chondrite parent body: Implications for metamorphic grade and accretionary time-scales. *Geochim. Cosmochim. Acta, 119,* 302.
Morbidelli A., Chambers J., Lunine J. I., et al. (2000) Source regions and time scales for the delivery of water to Earth. *Meteoritics & Planet. Sci., 35,* 1309.
Morbidelli A., Bottke W. F., Nesvorný D., et al. (2009) Asteroids were born big. *Icarus, 204,* 558.
Morfill G. E., Durisen R. H., and Turner G. W. (1998) NOTE: An accretion rim constraint on chondrule formation theories. *Icarus, 134,* 180.
Mostefaoui S., Lugmair G. W., and Hoppe P. (2005) ^{60}Fe: A heat source for planetary differentiation from a nearby supernova explosion. *Astrophys. J., 625,* 271.
Mothé-Diniz T. and Nesvorný D. (2008) Visible spectroscopy of extremely young asteroid families. *Astron. Astrophys., 486,* L9.
Mothé-Diniz T., Roig F., and Carvano J. M. (2005) Reanalysis of asteroid families structure through visible spectroscopy. *Icarus, 174,* 54.
Mothé-Diniz T., Carvano J. M., Bus S. J., et al. (2008) Mineralogical analysis of the Eos family from near-infrared spectra. *Icarus, 195,* 277.
Nakagawa Y., Sekiya M., and Hayashi C. (1986) Settling and growth of dust particles in a laminar phase of a low-mass solar nebula. *Icarus, 67,* 375.
Nelson R. P. and Gressel O. (2010) On the dynamics of planetesimals embedded in turbulent protoplanetary discs. *Mon. Not. R. Astron. Soc., 409,* 639.
Nelson R. P. and Papaloizou J. C. B. (2004) The interaction of giant planets with a disc with MHD turbulence — IV. Migration rates of embedded protoplanets. *Mon. Not. R. Astron. Soc., 350,* 849.
Nelson V. E. and Rubin A. E. (2002) Size-frequency distributions of chondrules and chondrule fragments in LL3 chondrites: Implications for parent-body fragmentation of chondrules. *Meteoritics & Planet. Sci., 37,* 1361.
Nelson R. P., Gressel O., and Umurhan O. M. (2013) Linear and non-linear evolution of the vertical shear instability in accretion discs. *Mon. Not. R. Astron. Soc., 435,* 2610.
O'Brien D. P., Walsh K. J., Morbidelli A., et al. (2014) Water delivery and giant impacts in the "Grand Tack" scenario. *Icarus, 239,* 74.
Oishi J. S., Mac Low M.-M., and Menou K. (2007) Turbulent torques on protoplanets in a dead zone. *Astrophys. J., 670,* 805.
Okuzumi S., Tanaka H., Kobayashi H., et al. (2012) Rapid coagulation of porous dust aggregates outside the snow line: A pathway to successful icy planetesimal formation. *Astrophys. J., 752,* 106.
Ormel C. W. and Cuzzi J. N. (2007) Closed-form expressions for particle relative velocities induced by turbulence. *Astron. Astrophys., 466,* 413.
Ormel C. W. and Klahr H. H. (2010) The effect of gas drag on the growth of protoplanets. Analytical expressions for the accretion of small bodies in laminar disks. *Astron. Astrophys., 520,* A43.
Ormel C. W. and Okuzumi S. (2013) The fate of planetesimals in turbulent disks with dead zones. II. Limits on the viability of runaway accretion. *Astrophys. J., 771,* 44.
Ormel C. W., Cuzzi J. N., and Tielens A. G. G. M. (2008) Co-accretion of chondrules and dust in the solar nebula. *Astrophys. J., 679,* 1588.
Ouellette N., Desch S. J., and Hester J. J. (2007) Interaction of supernova ejecta with nearby protoplanetary disks. *Astrophys. J., 662,* 1268.
Palme H. and Jones A. (2005) Solar system abundances of the elements. In *Treatise on Geochemistry, Vol. 1: Meteorites, Comets and Planets* (A. M. Davis, ed.), pp. 41–60. Elsevier, Amsterdam.
Pan M. and Sari R. (2005) Shaping the Kuiper belt size distribution by shattering large but strengthless bodies. *Icarus, 173,* 342.
Pan L., Padoan P., Scalo J., et al. (2011) Turbulent clustering of protoplanetary dust and planetesimal formation. *Astrophys. J., 740,* 6.
Pan L., Desch S. J., Scannapieco E., et al. (2012) Mixing of clumpy supernova ejecta into molecular clouds. *Astrophys. J., 756,* 102.
Quitté G., Halliday A. N., Meyer B. S., et al. (2007) Correlated iron 60, nickel 62, and zirconium 96 in refractory inclusions and the origin of the solar system. *Astrophys. J., 655,* 678.
Quitté G., Latkoczy C., Schönbächler M., et al. (2011) ^{60}Fe-^{60}Ni systematics in the eucrite parent body: A case study of Bouvante and Juvinas. *Geochim. Cosmochim. Acta, 75,* 7698.
Raymond S. N., Quinn T., and Lunine J. I. (2004) Making other Earths: Dynamical simulations of terrestrial planet formation and water delivery. *Icarus, 168,* 1.
Ros K. and Johansen A. (2013) Ice condensation as a planet formation mechanism. *Astron. Astrophys., 552,* A137.
Rubin A. E. (2000) Petrologic, geochemical and experimental constraints on models of chondrule formation. *Earth Sci. Rev., 50,* 3.
Rubin A. E. (2005) Relationships among intrinsic properties of ordinary chondrites: Oxidation state, bulk chemistry, oxygen isotopic composition, petrologic type, and chondrule size. *Geochim. Cosmochim. Acta, 69,* 4907.
Rubin A. E. (2011) Origin of the differences in refractorylithophile-element abundances among chondrite groups. *Icarus, 213,* 547.
Rubin A. E. and Brearley A. J. (1996) A critical evaluation of the evidence for hot accretion. *Icarus, 124,* 86.
Schneider D. M., Akridge D. G., and Sears D. W. G. (1998) Size distribution of metal grains and chondrules in enstatite chondrites. *Meteoritics & Planet. Sci., Suppl., 33,* 136.
Schräpler R., Blum J., Seizinger A., et al. (2012) The physics of protoplanetesimal dust agglomerates. VII. The low-velocity collision behavior of large dust agglomerates. *Astrophys. J., 758,* 35.
Scott E. R. D. and Krot A. N. (2003) Chondrites and their components. In *Treatise on Geochemistry, Vol. 1: Meteorites, Comets and Planets* (A. M. Davis, ed.), p. 143. Elsevier, Amsterdam.
Scott E. R. D. and Rajan R. S. (1981) Metallic minerals, thermal histories and parent bodies of some xenolithic, ordinary chondrite meteorites. *Geochim. Cosmochim. Acta, 45,* 53.
Scott E. R. D., Rubin A. E., Taylor G. J., et al. (1984) Matrix material in type 3 chondrites — Occurrence, heterogeneity and relationship with chondrules. *Geochim. Cosmochim. Acta, 48,* 1741.
Scott E. R. D., Krot T. V., Goldstein J. I., et al. (2014) Thermal and impact history of the H chondrite parent asteroid during metamorphism: Constraints from metallic Fe-Ni. *Geochim. Cosmochim. Acta, 136,* 13.
Sekiya M. (1983) Gravitational instabilities in a dust-gas layer and formation of planetesimals in the solar nebula. *Progr. Theor. Phys. Suppl., 69*, 1116.
Setoh M., Hiraoka K., Nakamura A. M., et al. (2007) Collisional disruption of porous sintered glass beads at low impact velocities. *Adv. Space Res., 40,* 252.
Shaw R. (2003) Particle-turbulence interactions in atmospheric clouds. *Annu. Rev. Fluid Mech., 35,* 183–227.
Shukolyukov A. and Lugmair G. W. (1993) Live iron-60 in the early solar system. *Science, 259,* 1138.
Simon J. B., Beckwith K., and Armitage P. J. (2012) Emergent mesoscale phenomena in magnetized accretion disc turbulence. *Mon. Not. R. Astron. Soc., 422,* 2685.
Sirono S.-i. (2011) Planetesimal formation induced by sintering. *Astrophys. J. Lett., 733,* L41.
Sonett C. P. and Colburn D. S. (1968) Electrical heating of meteorite parent bodies and planets by dynamo induction from a pre-main sequence T Tauri "solar wind." *Nature, 219,* 924.
Squires K. D. and Eaton J. K. (1990) Particle response and turbulence modification in isotropic turbulence. *Phys. Fluids, 2,* 1191.
Squires K. D. and Eaton J. K. (1991) Preferential concentration of particles by turbulence. *Phys. Fluids, 3,* 1169.

Stewart S. T. and Leinhardt Z. M. (2009) Velocity-dependent catastrophic disruption criteria for planetesimals. *Astrophys. J. Lett., 691,* L133.
Tachibana S. and Huss G. R. (2003) The initial abundance of ^{60}Fe in the solar system. *Astrophys. J. Lett., 588,* L41.
Tachibana S., Huss G. R., Kita N. T., et al. (2006) ^{60}Fe in chondrites: Debris from a nearby supernova in the early solar system? *Astrophys. J. Lett., 639,* L87.
Tang H. and Dauphas N. (2012) Abundance, distribution, and origin of ^{60}Fe in the solar protoplanetary disk. *Earth Planet. Sci. Lett., 359,* 248.
Tang X. and Chevalier R. A. (2014) Gamma-ray emission from supernova remnant interactions with molecular clumps. *Astrophys. J. Lett., 784,* L35.
Tatischeff V., Duprat J., and de Séréville N. (2010) A runaway Wolf-Rayet star as the origin of ^{26}Al in the early solar system. *Astrophys. J. Lett., 714,* L26.
Taylor G. J., Maggiore P., Scott E. R. D., et al. (1987) Original structures, and fragmentation and reassembly histories of asteroids - Evidence from meteorites. *Icarus, 69,* 1.
Telus M., Huss G. R., Ogliore R. C., et al. (2012) Recalculation of data for short-lived radionuclide systems using less-biased ratio estimation. *Meteoritics & Planet. Sci., 47,* 2013.
Testi L., Birnstiel T., Ricci L., et al. (2014) Dust evolution in protoplanetary disks. In *Protostars and Planets VI* (H. Beuther et al., eds.), pp. 339–362. Univ. of Arizona, Tucson.
Trieloff M., Jessberger E. K., Herrwerth I., et al. (2003) Structure and thermal history of the H-chondrite parent asteroid revealed by thermochronometry. *Nature, 422,* 502.
Trinquier A., Elliott T., Ulfbeck D., et al. (2009) Origin of nucleosynthetic isotope heterogeneity in the solar protoplanetary disk. *Science, 324,* 374.
Turner N. J., Fromang S., Gammie C., et al. (2014) Transport and accretion in planet-forming disks. In *Protostars and Planets VI* (H. Beuther et al., eds.), pp. 411–432. Univ. of Arizona, Tucson.
Urey H. C. (1955) The cosmic abundances of potassium, uranium, and thorium and the heat balances of the Earth, the Moon, and Mars. *Proc. Natl. Acad. Sci., 41,* 127.
Vasileiadis A., Nordlund Å., and Bizzarro M. (2013) Abundance of ^{26}Al and ^{60}Fe in evolving giant molecular clouds. *Astrophys. J. Lett., 769,* L8.
Vernazza P., Zanda B., Binzel R. P. et al. (2014) Multiple and fast: The accretion of ordinary chondrite parent bodies. *Astrophys. J., 791,* 120.
Villeneuve J., Chaussidon M., and Libourel G. (2012) Lack of relationship between aluminum-26 ages of chondrules and their mineralogical and chemical compositions. *Compt. Rend. Geosci., 344,* 423.
Voelk H. J., Jones F. C., Morfill G. E., et al. (1980) Collisions between grains in a turbulent gas. *Astron. Astrophys., 85,* 316.
Wada K., Tanaka H., Suyama T., et al. (2009) Collisional growth conditions for dust aggregates. *Astrophys. J., 702,* 1490.
Wada K., Tanaka H., Okuzumi S., et al. (2013) Growth efficiency of dust aggregates through collisions with high mass ratios. *Astron. Astrophys., 559,* A62.
Walsh K. J., Morbidelli A., Raymond S. N., et al. (2011) A low mass for Mars from Jupiter's early gas-driven migration. *Nature, 475,* 206.
Wang L.-P. and Maxey M. R. (1993) Settling velocity and concentration distribution of heavy particles in homogeneous isotropic turbulence. *J. Fluid Mech., 256,* 27.
Wasserburg G. J.,Wimpenny J., and Yin Q.-Z. (2012) Mg isotopic heterogeneity, Al-Mg isochrons, and canonical ^{26}Al/^{27}Al in the early solar system. *Meteoritics & Planet. Sci., 47,* 1980.
Wasson J. T., Isa J., and Rubin A. E. (2013) Compositional and petrographic similarities of CV and CK chondrites: A single group with variations in textures and volatile concentrations attributable to impact heating, crushing and oxidation. *Geochim. Cosmochim. Acta, 108,* 45.
Weidenschilling S. J. (1977a) Aerodynamics of solid bodies in the solar nebula. *Mon. Not. R. Astron. Soc., 180,* 57.
Weidenschilling S. J. (1977b) Aerodynamics of solid bodies in the solar nebula. *Mon. Not. R. Astron. Soc., 180,* 57.
Weidenschilling S. J. (2011) Initial sizes of planetesimals and accretion of the asteroids. *Icarus, 214,* 671.
Weidling R., Güttler C., and Blum J. (2012) Free collisions in a microgravity many-particle experiment. I. Dust aggregate sticking at low velocities. *Icarus, 218,* 688.
Weisberg M. K., McCoy T. J., and Krot A. N. (2006) Systematics and evaluation of meteorite classification. In *Meteorites and the Early Solar System II* (D. S. Lauretta and H. Y. McSween, Jr., eds.), pp. 19–52. Univ. of Arizona, Tucson.
Weiss B. P. and Elkins-Tanton L. T. (2013) Differentiated planetesimals and the parent bodies of chondrites. *Annu. Rev. Earth Planet. Sci., 41,* 529.
Weiss B. P., Gattacceca J., and Stanley S. et al. (2010) Paleomagnetic records of meteorites and early planetesimal differentiation. *Space Sci. Rev., 152,* 341.
Whattam S. A., Hewins R. H., Cohen B. A., et al. (2008) Granoblastic olivine aggregates in magnesian chondrules: Planetesimal fragments or thermally annealed solar nebula condensates? *Earth Planet. Sci. Lett., 269,* 200.
Whipple F. L. (1972) On certain aerodynamic processes for asteroids and comets. In *From Plasma to Planet* (A. Elvius, ed.), p. 211. Wiley, New York.
Williams J. P. and Gaidos E. (2007) On the likelihood of supernova enrichment of protoplanetary disks. *Astrophys. J. Lett., 663,* L33.
Windmark F., Birnstiel T., Güttler C., et al. (2012a) Planetesimal formation by sweep-up: How the bouncing barrier can be beneficial to growth. *Astron. Astrophys., 540,* A73.
Windmark F., Birnstiel T., Ormel C. W., et al. (2012b) Breaking through: The effects of a velocity distribution on barriers to dust growth. *Astron. Astrophys., 544,* L16.
Wood J. A. (2005) The chondrite types and their origins. In *Chondrites and the Protoplanetary Disk* (A. N. Krot et al, eds.), p. 953. ASP Conf. Series 341, Astronomical Society of the Pacific, San Francisco.
Woosley S. E. and Heger A. (2007) Nucleosynthesis and remnants in massive stars of solar metallicity. *Phys. Rept., 442,* 269.
Wurm G., Paraskov G., and Krauss O. (2005) Growth of planetesimals by impacts at ~25 m/s. *Icarus, 178,* 253.
Xie J.-W., Payne M. J., Thébault P., et al. (2010) From dust to planetesimal: The snowball phase? *Astrophys. J., 724,* 1153.
Yang C.-C. and Johansen A. (2014) On the feeding zone of planetesimal formation by the streaming instability. *Astrophys. J., 792,* 86.
Yang C.-C., Mac Low M.-M., and Menou K. (2012) Planetesimal and protoplanet dynamics in a turbulent protoplanetary disk: Ideal stratified disks. *Astrophys. J., 748,* 79.
Youdin A. N. and Goodman J. (2005) Streaming instabilities in protoplanetary disks. *Astrophys. J., 620,* 459.
Youdin A. and Johansen A. (2007) Protoplanetary disk turbulence driven by the streaming instability: Linear evolution and numerical methods. *Astrophys. J., 662,* 613.
Youdin A. N. and Shu F. H. (2002) Planetesimal formation by gravitational instability. *Astrophys. J., 580,* 494.
Young E. D. (2014) Inheritance of solar short- and long-lived radionuclides from molecular clouds and the unexceptional nature of the solar system. *Earth Planet. Sci. Lett., 392,* 16.
Zanda B., Humayun M., and Hewins R. H. (2012) Chemical composition of matrix and chondrules in carbonaceous chondrites: Implications for disk transport. *Lunar Planet. Sci. XLIII,* Abstract #2413. Lunar and Planetary Institute, Houston.
Zinner E. and Göpel C. (2002) Aluminum-26 in H4 chondrites: Implications for its production and its usefulness as a fine-scale chronometer for early solar system events. *Meteoritics & Planet. Sci., 37,* 1001.
Zsom A., Ormel C. W., Güttler C., et al. (2010) The outcome of protoplanetary dust growth: Pebbles, boulders, or planetesimals? II. Introducing the bouncing barrier. *Astron. Astrophys., 513,* A57.